國 立 交 通 大 學

機 械 工 程 學 系

博士論文

應用力控制與混合控制於前方腰椎椎間融合器與人工椎間盤之有限元素分析

Load- and Hybrid-Controlled Finite Element Analyses on Anterior Lumbar Interbody Fusion Cage and Artificial Disc

研 究 生：鍾政成

指導教授：洪景華 教授

中 華 民 國 九 十 八 年 八 月

應用力控制與混合控制於前方腰椎椎間融合器與人工椎間盤之有限元素分析

Load- and Hybrid-Controlled Finite Element Analyses on Anterior Lumbar Interbody Fusion Cage and Artificial Disc

研 究 生: 鍾政成　　Student: Zheng-Cheng Zhong

指導教授: 洪景華　　Advisor: Chinghua Hung

國立交通大學
機械工程學系
博士論文

A Thesis
Submitted to Department of Mechanical Engineering
College of Engineering
National Chiao Tung University
in Partial Fulfillment of the Requirements
for the Degree of
Doctor of Philosophy
in

Mechanical Engineering

August 2009

Hsinchu, Taiwan, Republic of China

中華民國九十八年八月

Load- and Hybrid-Controlled Finite Element Analyses on Anterior Lumbar Interbody Fusion Cage and Artificial Disc

Student: Zheng-Cheng Zhong Advisor: Dr. Chinghua Hung

Department of Mechanical Engineering

National Chiao Tung University

ABSTRACT

Recently, design concepts of spinal implants have changed from traditional stable fusion cages to mobile non-fusion artificial discs that attempt to restore normal physiological motion and lessen the deterioration of adjacent tissue. Several spinal testing protocols have been proposed to evaluate the biomechanical difference between these spinal implants, of which the load control method (LCM) and the new hybrid control method (HCM) are most popular worldwide. However, it is still not clear whether the LCM or the HCM should be preferentially used in evaluating the actual characteristics of spinal implants. This study used finite element (FE) analysis with the LCM and the HCM to analyze differences in range of motion (ROM), facet joint forces, and disc annulus stress at the implant and in adjacent levels after implantation of an anterior lumbar interbody fusion cage or an artificial disc.

A 3-dimensional, five-level intact lumbar spine FE model was constructed using Ansys 9.0 software. At the L3-L4 level, the intact model was modified to construct surgery models, including an artificial disc replacement (ADR) with ProDisc II, and an anterior lumbar interbody fusion (ALIF) with cage plus

pedicle screw fixation. The LCM imposed 10 N-m moments for each four physiological motions and a 150 N preload at the top of L1. The HCM process was otherwise in accordance with the standard hybrid testing protocol. The detailed ROMs are 16.84° in flexion, 14.73° in extension, 9.48° in torsion, and 17.14° in lateral bending, respectively.

At the implant level, this study suggests that both control methods can be adopted to predict the behavior of a fusion model, and similar stabilization characteristics can be found with both methods. The LCM emphasized the effects of the non-fusion device at the implant level. At adjacent levels, the HCM emphasized the effects of the fusion device. By comparing present data with clinical findings, the LCM was found to be more effective and clinically relevant in evaluating the accelerative degeneration of facet joints at the implant level after the insertion of an artificial disc. The HCM was more effective and clinically relevant in evaluating accelerative degeneration of discs and facet joints at adjacent levels after the insertion of a spinal cage. In addition, this study demonstrates that the use of stress distribution patterns to predict adjacent disc degeneration produces better results than ROM, especially in cases of total disc replacement.

This study suggests that these two analytical methods can be used to predict specific conditions in a patient's daily life. The HCM is suitable for evaluation of the patient's daily life motions during recovery and restoration of function after surgery. The LCM is suitable for evaluation of the patient's normal lift work-loading conditions after surgery.

Keywords: load control method, hybrid control method, finite element analysis, adjacent segment effect, interbody fusion cage, artificial disc

應用力控制與混合控制於前方腰椎椎間融合器與人工椎間盤之有限元素分析

研究生：鍾政成　　指導教授：洪景華

國立交通大學機械工程學系

摘　　要

近年來，脊椎植入物的設計概念已經從傳統的提供患處穩定性(融合器)逐漸轉為恢復可動性(人工椎間盤)；冀望在手術後可以使患處恢復正常的生理運動行為，以避免鄰近端的軟組織加速退化病變。各式的測試方法也被提出來評估這些脊椎植入物的生物力學差異；其中以力控制與混合控制兩種施力方法比較受到生物力學學者的接受。然而，對於使用力控制或是混合控制來評估脊椎植入物可能導致的差異仍不明確。本研究希望透過有限元素分析搭配力控制以及混合控制兩種施力方法來評估前方腰椎椎間融合器與人工椎間盤在置入腰椎後對手術端以及鄰近端椎節影響。評估參數包含有運動範圍、小面關節接觸力以及手術鄰近端環帶的應力分布。

本研究透過 Ansys 9.0 有限元素分析軟體建構出一個三維的五節腰椎有限元素模型(INT)。依據臨床手術方式，將上述兩植入物放入腰椎第三與第四椎節之間，以分別建立出 360 度椎間融合模型(ALIF)以及椎間盤置換模型(ADR)。力控制的施加方式是施加 150 牛頓的預負荷以及 10 牛頓-米的彎曲力矩來模擬前彎、後彎、扭轉與側彎動作。而混合控制的施力方式則是施加 150 牛頓的預負荷，並參考標準測試法分別對前彎，後彎、扭轉與側彎動作施加約 16.84 度、14.73 度、9.48 度與 17.14 度的運動範圍。

就手術端而言，本研究建議兩種施力方式都可以用來預測 ALIF 模型的手術端穩定性；而力控制施力法會強調 ADR 模型的手術端影響。就鄰近端而言，混合控制施力法則會明顯指出 ALIF 模型對鄰近端的影響。若將目前研究結果與臨床發現相比較可以發現，力控制施力法比較有效的評估出椎間盤置換手術後手術端小面關節加速退化的病變；而混合控制則較有效的評估出椎間融合手術後鄰近端椎間盤與小面關節加速退化的病變。此外，相較於單純使用運動範圍來評估鄰近端椎間盤退化問題，使用應力分布的差異來評估鄰近端椎間盤退化病變是更好的方式，尤其是在評估人工椎間盤的影響時。

本研究認為兩種施力方法皆能被用來預測病患在日常生活的特別情形。混合控制法適合用來評估病患在術後的日常生活動作行為。而力控制法適合用來評估病患在術後的日常工作受力行為。

關鍵字：力控制法、混合控制法、有限元素分析、鄰近椎節影響、椎間融合器、人工椎間盤

Acknowledgements

I would like to express my deepest gratitude and sincerest appreciation to my adviser, Professor Chinghua Hung (洪景華), for his encouragement, guidance and instruction during the period of this research. I also want to thank him for his patience and endurance of my carelessness.

I would like to express my gratitude to the member of my advisory and examination committee, Dr. Shih-Hao Chen (陳世豪), for his insight into the clinical aspects of this project – his expertise is greatly valued. I would also like to acknowledge the support of the other members of my examination committee: Dr. Chen-Sheng Chen (陳振昇), Dr. Jiann-Jong Liau (廖建忠), Dr. Shou-I Chen (陳守義), and Dr. Bing-Shiang Yang (楊秉祥), for their time and perspectives. This manuscript has grown as a result of their contributions.

I would like to thank my colleagues at the Precision Engineering & Simulation Laboratory for their kindly assistance and constructive suggestion in all respects. I will not forget any help that I received from members of Gear Research Laboratory and Optimization Design Laboratory. I would like to thank my roommates, Cristopher Camacho Leandro, Liang-Chi Chen (陳亮志), and Ching-Wen Lo (羅清文), for their help in the improvement of my English, and share with me in happiness, distress, everything, and "Tao"(道).

Most importantly I would like to deeply appreciate my soul mate and parents for their love, patience, and their constant encouragement to help me finishing this dissertation.

-- Zheng-Cheng Zhong (鍾政成)

Table of Contents

List of Tables

List of Figures

Chapter 1: Introduction

Spinal diseases are becoming more and more serious and dangerous for the human population. Approximately 70-85% of the population experiences back pain at some point in their lives [1]. In the United States, Medicare spending for back surgery increased from $500 million to $1 billion between 1992 and 2003 [2]. These diseases cost large amount of medical resources, and add huge encumbrances to our society.

1.1. Motivation and Objectives

The spinal fusion procedure is an effective and popular surgical technique for treating low back pain related to degenerative disc disease. However, the fusion procedure has been frequently associated with the postoperative long-term complication of adjacent segment degeneration, resulting in the need for another fusion surgery at adjacent levels. This higher incidence of adjacent segment degeneration (ASD) disease has been reported when patient were treated with rigid transpedicular instrumentation [3].

Recently, the design concepts of spinal implants have changed from traditional stable fusion to mobile non-fusion that attempts to lessen the deterioration of adjacent elements. Artificial discs are one of the new non-fusion spinal implants that have been developed to restore normal physiological motion and to overcome the disadvantages of the fusion procedure. Short-term clinical reports indicate that artificial discs provide physiological range of motion (ROM) similar to that of the healthy spinal disc, and do so without provoking ASD disease [4]. However, the long-term outcomes of these patients are still not clear, and require further researches.

In order to understand the long-term complications of ASD disease, a number of biomechanical research studies have evaluated various spinal

implants, using an *in vitro* experimental test or finite element (FE) analysis. Reviewing the literature, several spinal testing protocols have been reported in the past three decades, of which the load control method (LCM) and the new hybrid control method (HCM) are the most popular worldwide. However, the results of evaluations of these spinal implants may be influenced due to the use of different spinal testing protocols. At present, few studies focus on the differences between testing protocols. Therefore, finding a better and more suitable testing method for the evaluation of long-term complications associated with various spinal implants at the implant and adjacent levels is a very important topic in this field.

In Taiwan, human cadaveric lumbar spine specimens are difficult to obtain for experimental studies. Therefore, the purpose of this study was to construct a three-dimensional FE model of a five-level intact lumbar spine, and thus to use FE analysis with the LCM or HCM to explore biomechanical differences, at the implant level and at adjacent levels, between the anterior lumbar interbody fusion (ALIF) and lumbar artificial disc replacement (ADR) devices. Eventually, the ROM, facet contact force, and stress distribution on an adjacent disc annulus were compared between the intact lumbar spine and both surgery models. The findings of this study may help researchers understand which testing protocol is suitable for probing the physical effects of spinal implants.

1.2. Outline

This dissertation is divided into six chapters. (1) Introduction: this chapter introduces the motivation, objectives, and outline of this dissertation. (2) Background: this chapter reviews the anatomy of the spine and its biomechanics, spinal pathology and treatments, fusion and non-fusion techniques, clinical outcomes and long-term complications of ASD after implantation of a lumbar interbody fusion cage or an artificial disc, development of spinal testing protocols, and the characteristics of *in vitro* tests versus FE simulations. (3)

Materials and Methods: this chapter includes FE modeling techniques for the five-level intact lumbar spine, anterior lumbar interbody fusion, and total disc replacement surgery models. In addition, the convergence test for the intact lumbar spine model, as well as boundary and loading conditions of the LCM and HCM, are also included in the chapter. (4) Results and Discussion: This chapter includes data on the intact lumbar spine and both surgery models under the LCM or the HCM. Differences between both spinal testing protocols in evaluating a spinal cage or disc arthroplasty are revealed and discussed. In addition, model limitations are also included in this chapter. (5) Conclusion and Future Work: final suggestions are provided for understanding which testing protocol is suitable for understanding the physical effects of spinal implants. In addition, several topics that can be extended from this research are introduced in this chapter.

Chapter 2: Background

The following sections contain a review of the anatomy of the spine, its biomechanics, spine pathology and treatments, fusion and non-fusion techniques, clinical outcomes after implantation of a lumbar interbody fusion cage or an artificial disc, development of spinal testing protocols, and the characteristics of *in vitro* tests versus FE simulations.

2.1. Spine Anatomy and Biomechanics

The vertebral column consists of 33 vertebrae divided into five regions (Figure 2.1). There are 7 cervical vertebrae, 12 thoracic vertebrae, 5 lumbar vertebrae, 5 fused sacral vertebrae, and 4 fused coccygeal vertebrae. In the cervical, thoracic, and lumbar regions, there are intervertebral discs between adjacent vertebrae to absorb shock and restrain excessive motion. Within these regions, two adjacent vertebrae and their intervening soft tissues are called a motion segment, which is a functional unit of the spine (Figure 2.2). The principal functions of the spine are to protect the spinal cord and transfer loads from the head and trunk to the pelvis.

2.1.1. Vertebrae

A typical vertebra consists of a body, a hollow ring, and several bony processes, such as the pedicle, lamina, spinous process, and transverse process, as shown in Figure 2.3(a). Each vertebral body consists of an outer shell of cortical bone and an inner core of cancellous bone. The vertical and horizontal structure of bone in the cancellous core is called trabecular bone (Figure 2.3(b)). Most of the compressive force acting down the long axis of the spine is resisted by the cancellous bone because of its dense network of trabecular bone [5]. In general, vertebral size progressively increases from the cervical region to the

lumbar region.

2.1.2. Intervertebral Disc

The intervertebral disc is composed of three parts: the nucleus pulposus, the annulus fibrosus, and two cartilaginous endplates (Figure 2.4). The nucleus pulposus is located in the centre of each disc and is only slightly compressible, with 80 to 88% water content [6]. In general, the lumbar nucleus fills 30 to 50% of the total cross-section disc area [7]. The annulus fibrosus consists of approximately 15-25 concentric lamellae in the circumference around the nucleus, each of which contains collagen fibers [8]. The collagen fibers are oriented at an approximately 30° angle to the horizontal plane and crisscross each other in the adjacent lamella. The superior and inferior cartilaginous endplates cover the disc and connect with adjacent vertebral bodies.

The primary function of the disc is to transfer compressive forces evenly from one vertebral body to the next, while allowing for small-amplitude twisting and sliding movements [9]. The tensile properties of the annulus are stiffer in anterior than the posterolateral regions, with the outer region being stiffer than the inner regions [10]. The outer lamellae resist excessive bending and twisting of adjacent vertebrae, while the innermost lamellae are deformable and normally behave like a fluid. The endplate not only helps to equalize loading of the vertebral body but also prevents rapid fluid loss from the nucleus [11].

2.1.3. Facet Joint

The facet joint is composed of the superior articular process, inferior articular process, and joint capsule. The joint capsule attaches to the superior and inferior articular processes. The orientation of the facet joints varies with the spinal region. In general, the facets of the lumbar spine are oriented at a 90° angle to the transverse plane and at a 45° angle to the frontal plane (Figure 2.5). They stabilize the lumbar spine during compression, and prevent excessive axial

torsion and forward sliding between vertebrae [12].

2.1.4. Spinal Ligaments

A number of ligaments support the spine, including anterior longitudinal ligament (ALL), posterior longitudinal ligament (PLL), ligamentum flavum (LF), interspinous ligament (ISL), supraspinous ligament (SSL), intertransverse ligament (TL), and capsular ligament (CL). The orientation of each ligament is shown in Figure 2.2. The primary function of these ligaments is to protect the spine by preventing excessive movement. The amount of strain on the various ligaments differs with the type of motion of the spine. The capsular ligaments of the facet joints bear the most strain during axial torsion [13].

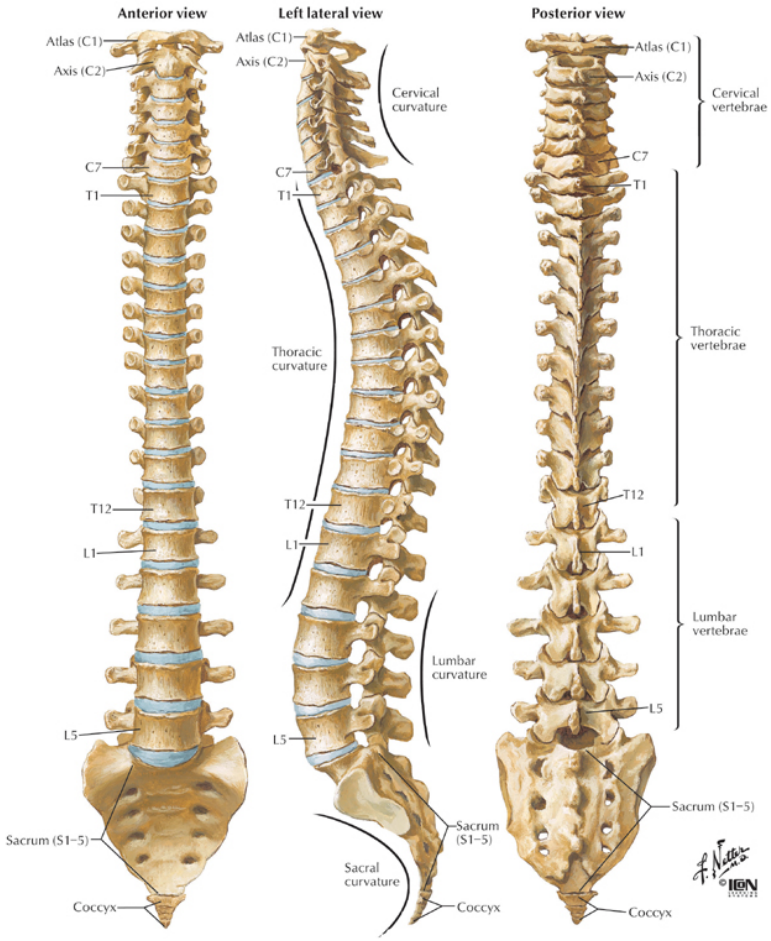

Figure 2.1: Vertebral column: anterior, left lateral and posterior views of the major regions of the spine.

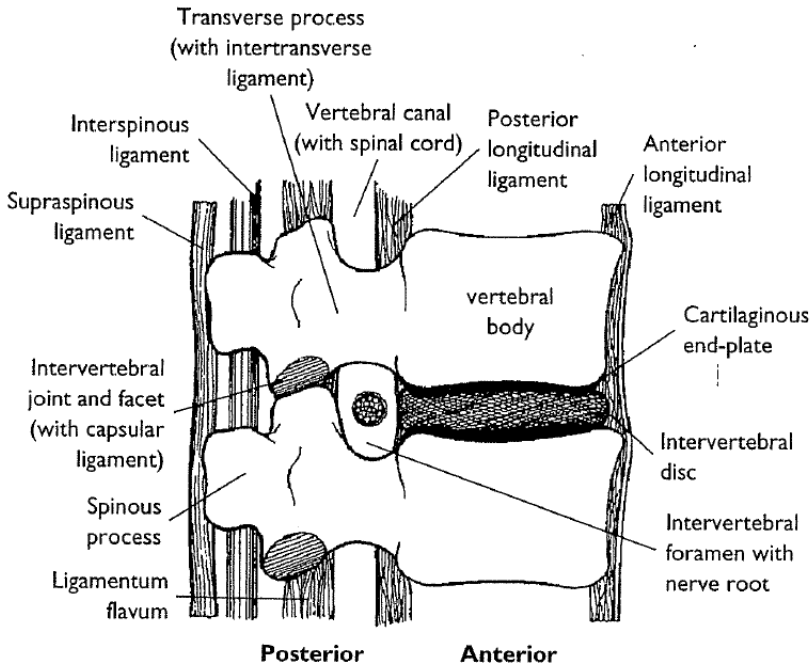

Figure 2.2: The motion segment in the lumbar spine, which is composed of two vertebrae and the surrounding soft tissue [14].

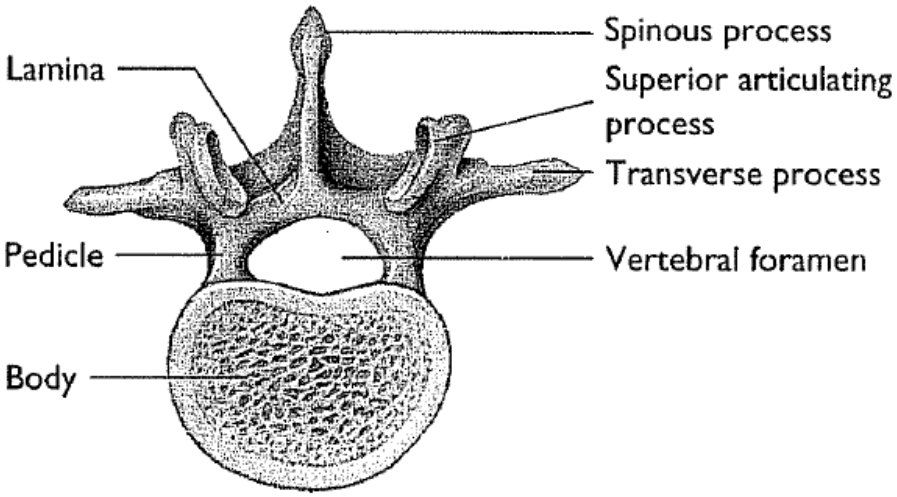

(a)

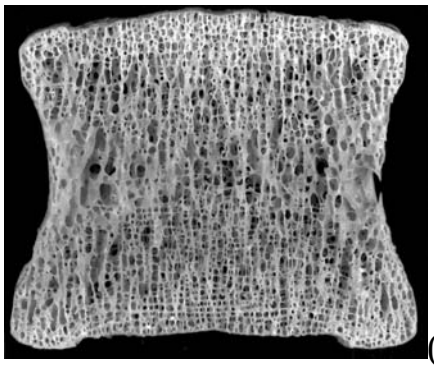

(b)

Figure 2.3: The shape of a human vertebra. (a) Superior view of the typical lumbar vertebra. (b) The trabecular structure of a lumbar vertebral body in sagittal section [14].

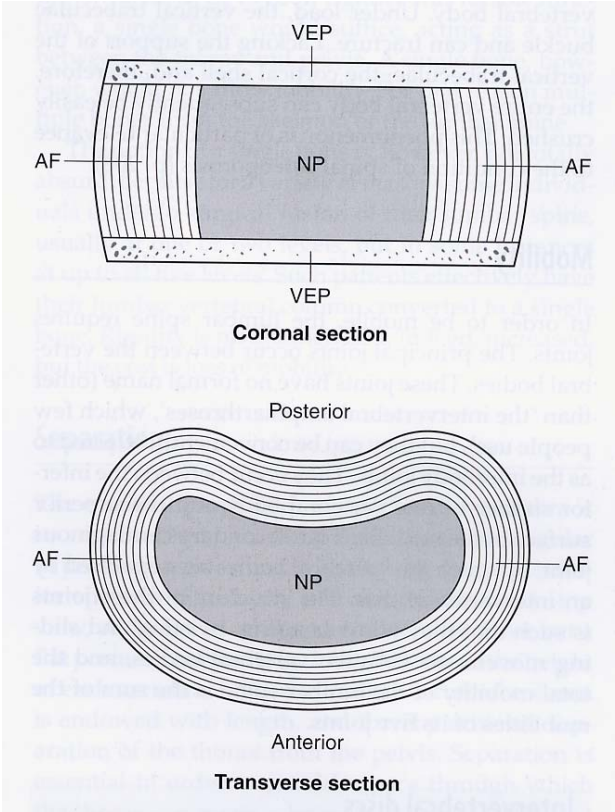

Figure 2.4: The structure of an intervertebral disc. The disc consists of the nucleus pulposus (NP), annulus fibrosus (AF), and two cartilaginous vertebral endplates (VEP) [9].

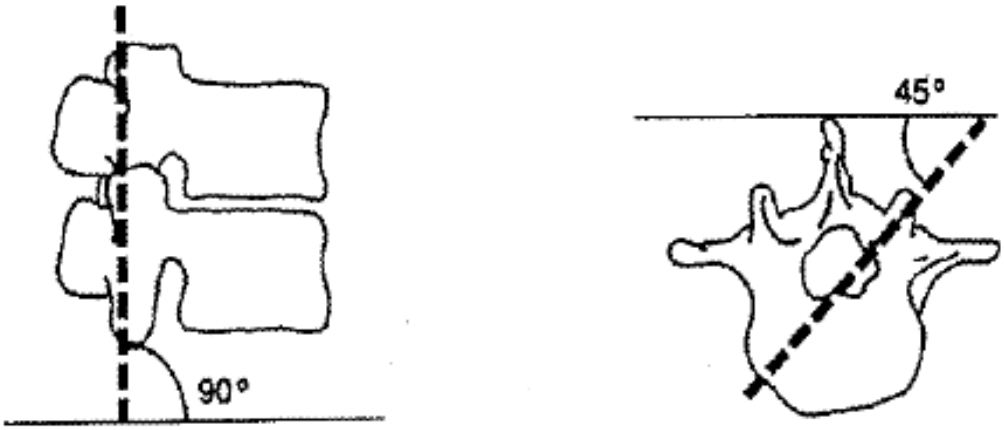

Figure 2.5: The orientation of lumbar facet to the transverse plane (left) and the frontal plane (right).

2.2. Spinal Pathology and Treatments

The functions of the spine are to provide longitudinal weight support, limit excessive movement, and protect the posterior spinal cord. However, spinal instability may be induced by severe pathological changes, such as degenerative disc disease, spinal deformity, tumor, infection, trauma, congenital anomaly, inflammation, etc. (Figure 2.6). Thus, spinal nerve roots or the spinal cord may be compressed, leading to limb paralysis or low back pain (Figure 2.7). The first choice of treatment for low back pain is conservative therapy, such as physical therapy or medication. When conservative treatments fail, spine surgeons may perform either fusion or non-fusion surgery, with the aim of reducing pain and decreasing disability [15].

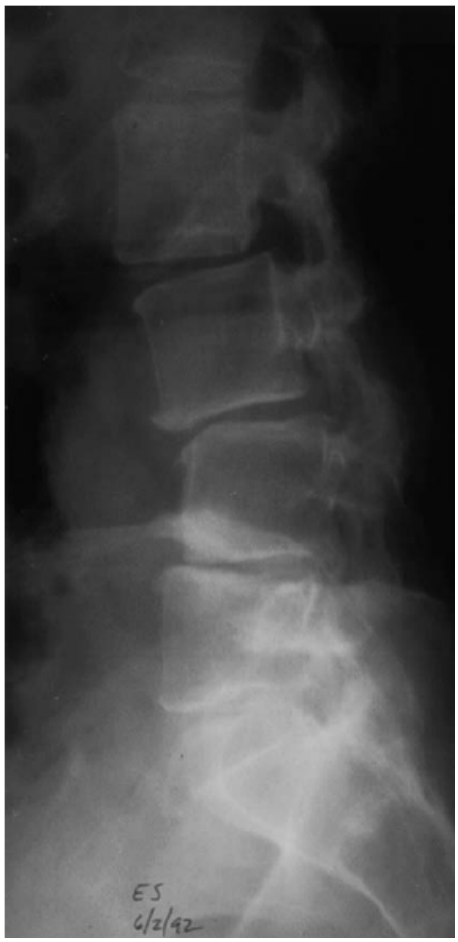

Figure 2.6: This radiograph shows spinal instability [16].

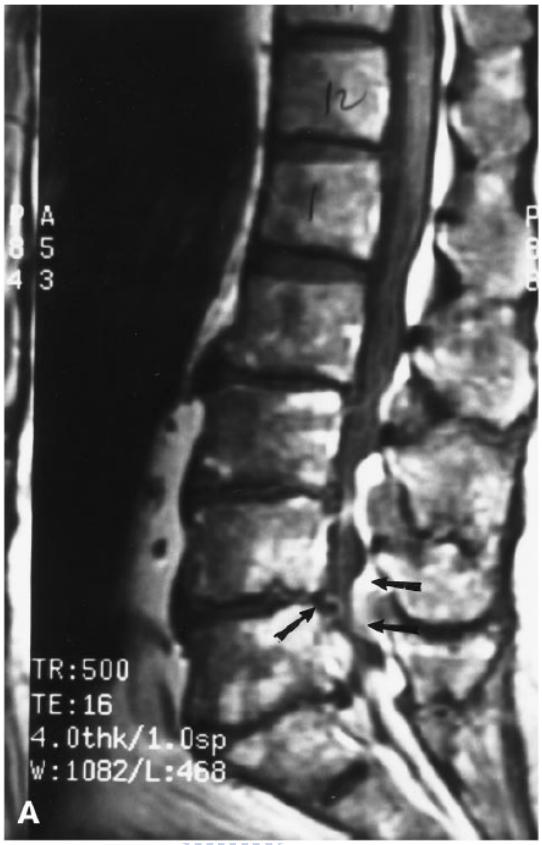

Figure 2.7: Magnetic resonance imaging (MRI) shows stenosis of the lumbar spine [17].

2.3. Spinal Fusion Techniques

The first report of spinal fusion was by Hibbs in 1911 [18]. Spinal fusion is defined as a bony union between two vertebrae spaces following surgical manipulation [19], and aims to completely eliminate movement by the motion segment (Figure 2.8). It is an effective technique for treating degenerative spinal instability, and the final goal of the procedure is to restore disc height, enlarge the stenotic foramen, and support the anterior spinal column. In general, bone grafts are placed into the interface between vertebral bodies to maintain disc height and to accelerate bone growth into neighboring vertebrae. These bone grafts may be autografts, allografts or synthetic materials which can be adopted from fibulae, illia, the iliac crest, or ribs.

Over the past 20 years, spinal fusion has become a very popular surgical technique for the treatment of low back pain caused by degenerative disc disorders. However, several of the complications of spinal fusion related to the use of bone grafts have been reported, such as high rate of graft collapse, spinal instability due to pseudarthrosis, deep infection at the donor site, and a low fusion rate using allografts [20]. Stauffer and Coventry [21] reported on 83 patients who had had an ALIF between 1959 and 1967. Only 36% of the 77 patients had good relief of pain for an average of 3.75 years of follow-up. In addition, the high rate of pseudarthrosis (44% of 68 patients) was evaluated radiographically at a minimum of 18 months' follow-up. Dennis *et al.* [22] measured the height of disc space preoperatively, early postoperatively, and at an average of 29 months postoperatively in each of the 31 patients who had had an ALIF with the use of an autograft or allograft. Although immediate postoperative radiographs showed an average increase of 9.5 mm (89% of disc height preoperatively) in the disc height, the use of a graft alone did not provide long-term distension of the disc space or increase neuroforaminal height. Disc height decreased in every patient at 29 months after the ALIF operation. Thus, the nerve roots may be compressed again, leading to radiculopathy. These

studies demonstrated that the use of an autograft or allograft alone cannot deliver acceptable and satisfactory clinical outcomes in a long-term follow-up. To avoid the disadvantages of spinal fusion with the use of a bone graft alone, the spinal interbody fusion cage was developed to overcome these problems.

The most common surgical techniques for the insertion of a spinal cage can be classified as the ALIF approach, posterior lumbar interbody fusion (PLIF) approach, and transforaminal lumbar interbody fusion (TLIF) approach. In general, the ALIF approach includes the removal of the ALL, the anterior portions of the disc annulus, and the nucleus before implanting an interbody fusion cage (Figure 2.9; black arrow) [23]. For the PLIF approach, a partial laminectomy, discectomy and nucleotomy are performed, which includes the removal of the ISL, SSL, LF, posterior portions of the disc annulus, and the total nucleus. In addition, a certain portion of the facet joint can be removed to give the nerve roots more space (Figure 2.9; red arrow) [24]. Recently, the TLIF approach has been proposed and modified from the PLIF method to provide a minimally invasive surgical (MIS) technique. After the spine is approached, an inferior hemilaminectomy and a unilateral facectomy are performed (Figure 2.9; blue arrow) [25]. In general, the additional posterior fixation is suggested in order to reconstruct a stable environment. When the ALIF is combined with posterior fixation, the process is called an anterior-posterior (AP) fusion or a 360° fusion. The choice of surgical approach for insertion of a spinal cage is related to instability at the fusion site or the indication of each patient; however, it also depends on which approach the spine surgeon is most comfortable using.

2.3.1. Spinal Interbody Fusion Cage

The spinal interbody fusion cage was developed by Bagby in the 1980s. It can replace the degenerative disc and distension the intervertebral body, thus restoring physiological disc height. In general, there are several features of this device (Figure 2.10). First, the spinal fusion cage is made of a variety of

biocompatible materials, including stainless steel, titanium alloy, carbon fiber-reinforced polymer (CFRP), and polyetheretherketone (PEEK) [20]. Due to the high mechanical strength of these materials, a spinal interbody fusion cage can provide better longitudinal support than a traditional bone graft, without causing collapse. Second, rough or specific designs can be found on the contact surfaces of spinal cages. In order to prevent cage slippage, rough contact surfaces, saw teeth, spikes or threads have been designed to increase stability between fusion devices and endplates. Third, these implants are usually designed to be hollow, with small pore or openings on the wall. These hollow cages can be filled with bone grafts to promote bone growth. Furthermore, only small amounts of cancellous bone are required, because there is no longer need for the cubic graft to be a spacer. The small pores and openings on the wall allow the growth of bone through the cage, resulting in bony fusion. Therefore, spinal fusion cages can avoid donor site morbidity and increase fusion rates.

Currently, many kinds of spinal cage designs are available on the market (Figure 2.10), which can be classified by the various surgical approaches used in their implantation. Large single lumbar cage designs are used for the ALIF procedure (Figure 2.10 (c) and (d)). Some paired cage designs are used strictly for PLIF procedures (Figure 2.10 (e), (f), (g) and (h)), while others can be inserted using either an ALIF or PLIF (Figure 2.10 (a) and (b)). In addition, some specific shapes of cages are designed for MIS techniques such as the TLIF procedure (Figure 2.10 (i)). Despite differences among these cage designs, most cage designs are suggested for use in combination with posterior fixation. However, the stand-alone cage was developed for the ALIF procedure, removing the need for an additional posterior fixation system (Figure 2.10 (d)).

At present, ALIF combined with posterior pedicle screw fixation can provide better stability than other fusion techniques. Therefore, SynCage-Open interbody cage supplementation with posterior pedicle screw fixation was selected to represent the fusion model in this study.

2.3.2. Clinical Outcomes Associated with Fusion Cages

Previously reported clinical series of lumbar interbody fusion cages have demonstrated favorable short-term outcomes (Table 2.1), with the successful fusion rate ranging between 91% and 96% [26-29]. Brantigan *et al.* [27] indicated that use of a rectangular spinal cage can restore and maintain disc height at a 2-year follow-up. Kuslich *et al.* [28] reported the 4-year follow-up results of a BAK lumbar cage. The results indicated that the fusion rate was slightly better in the one-level procedure than in the two-level procedure (100% vs. 95.7%). Furthermore, there was little difference in the fusion rate between the ALIF and the PLIF for one-level procedures. However, in two-level procedures, the fusion rate was 68.4% (13/19) for the PLIF group. Yuan *et al.* [29] reported that the types and rates of complications differed between the ALIF and PLIF approach with the use of a threaded cage. In general, dural tears (10.1% of 356 patients) were only related to the PLIF approach, whereas damage to major vessels, urological complications, and postoperative ileus (1.7, 1.4, and 2.2%, respectively, of 591 patients) were associated with the ALIF approach. Overall, a spinal cage can maintain disc height, provide a high rate of fusion, be used in either one-level or two-level procedures, and obtain similar clinical results with both the ALIF and PLIF approaches.

The 10-year long-term results of spinal cage implantation have been reported by Brantigan *et al.* [16]. This study indicated that patient satisfaction was reached in 93.9% (31 of 37 patients) of patients. However, a high incidence of ASD was found. ASD occurred in 61% of patients, but was clinically significant in only 20%. Anjarwalla *et al.* [30] indicated that the use of pedicle screw stabilization with ALIF produced a significant increase in the rate of interbody fusion (from 51% up to 88%). Park *et al.* [3] reviewed reports in the literature of ASD disease after spinal fusion between 1966 and 2002, following the use of either a spinal cage or a bone graft. The incidence of ASD was higher

in patients with pedicle screw instrumentation (12.2–18.5%) compared to patients fused with other forms of instrumentation or with no instrumentation (5.2–5.6%).

In general, whether using a spinal cage or a bone graft, the long-term complications of ASD disease may be induced because various spinal fusions restrain motion at the surgical level [28, 31, 32]. Although the additional use of posterior pedicle screw instrumentation can increase the fusion rate [30], it also has been shown to increase the incidence of ASD disease (Figure 2.11) [3, 16, 33-35]. Clinical studies have reported incidence rates ranging from 5.2% to 61%, as shown in Table 2.1. Therefore, non-fusion spinal implants were developed to avoid ASD disease.

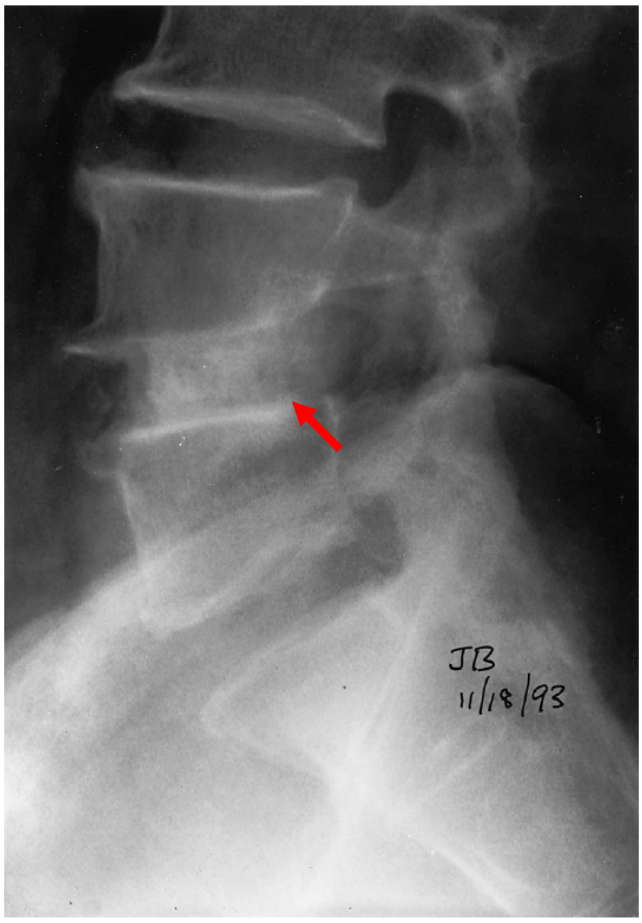

Figure 2.8: This radiograph demonstrates a solid bony union between L3 and L4 [27].

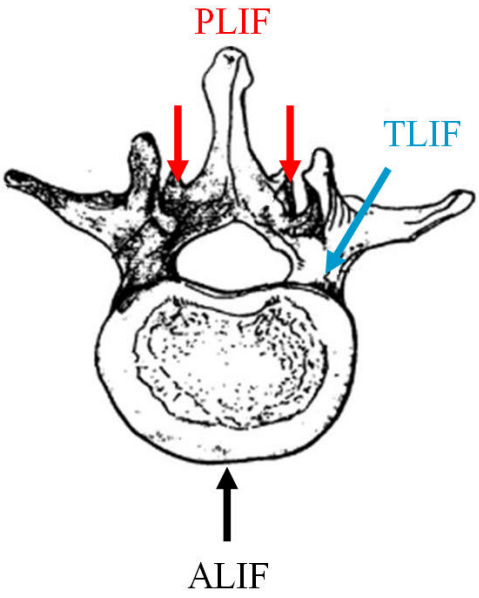

Figure 2.9: Common surgical techniques for insertion of a spinal cage. The black arrow indicates the ALIF approach, the red arrow indicates the PLIF approach, and the blue arrow indicates the TLIF approach.

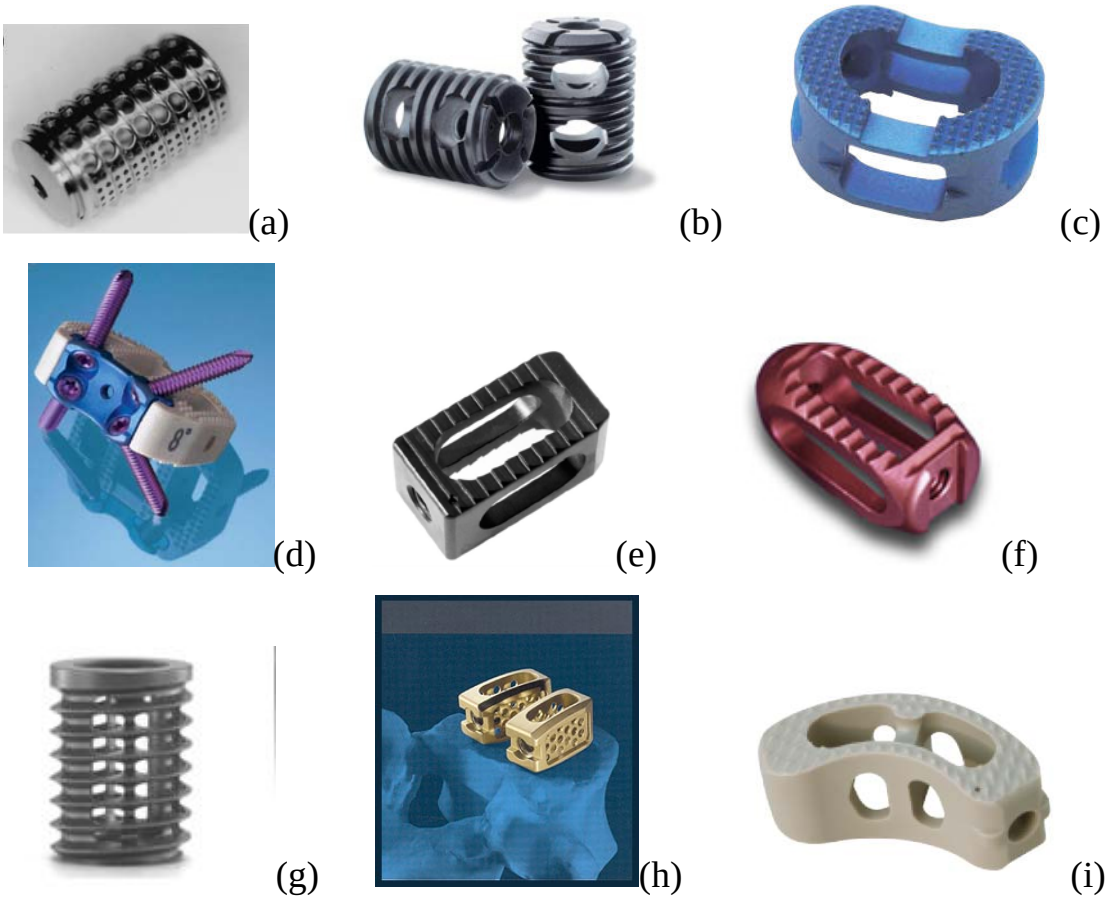

Figure 2.10: Various lumbar interbody fusion cages: (a)TIBFD (Medtronic Sofamor-Danek, Inc., Memphis, Tennessee, USA); (b) BAK (Sulzer Spine-Tech Inc., Minneapolis, Minnesota, USA); (c) SynCage-Open (Synthes Spine, Inc., Mathys Medical Ltd., Bettlach, Switzerland); (d) SynFix (Synthes Spine, Inc., Mathys Medical Ltd., Bettlach, Switzerland); (e) posterior lumbar Brantigan I/F (Depuy-AcroMed Corp., Cleveland, Ohio, USA); (f) O.I.C. (Stryker Spine, Mahwah, New Jersey, USA); (g) Ray-TFC (Surgical Dynamics, Norwalk, Connecticut, USA); (h) Contact Fusion Cage (Stratec Medical Ltd., Oberdorf, Switzerland); (i) AVS-TL (Stryker Spine, Mahwah, New Jersey, USA).

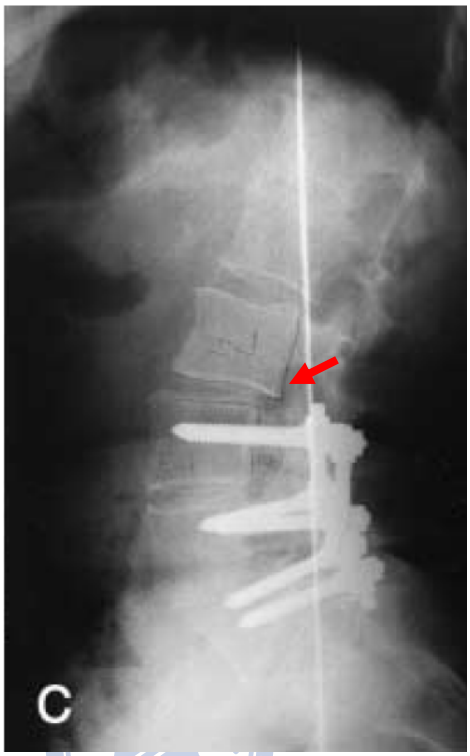

Figure 2.11: Adjacent segment degeneration disease developed at L2/3 after 5-year spinal fusion [36].

Table 2.1: Clinical outcomes of lumbar interbody fusion cages

Authors	Purpose	Follow-up/Approach	Outcome
Ray (1997) [26]	To evaluate the safety and effectiveness of the Ray threaded fusion cage	6-48 months / PLIF	*Fusion rate: 96% of 208 patients
Kuslich *et al.* (2000) [28]	To determine the early clinical results in fusion with BAK cage	4-year / ALIF and PLIF	* Fusion rate: 95.1% of 196 patients *Fusion rate (one-level vs. two-level): 100% vs. 95.7% *No difference between ALIF and PLIF, except in two-level procedures with PLIF * ASD: 5.6%
Brantigan *et al.* (2000) [27]	To determine the early results of patients who received Brantigan I/F cage	2-year / PLIF with posterior fixation	*Fusion rate: 98.9% of 178 patients *Average disc space height (pre- vs. postoperation): 7.9 mm vs. 12.3 mm *Fusion success was not diminished over multiple fusion levels. *Screw breakage: 5.9% (13 of 221 patients)
Yuan *et al.* (1997) [29]	Clinical trial of the BAK cage	2-year / ALIF and PLIF	*Fusion rate: 91% of 283 patients *Complications related to the PLIF: dural tears (10.1% of 356 patients) *Complications related to the ALIF: damage to major vessels, urological complications, and postoperative ileus (1.7, 1.4, and 2.2%, respectively, of 591 patients)
Anjarwalla *et al.* (2006) [30]	To assess the effect of different types of posterior stabilization on the fusion rate of ALIF	At least 2-year / ALIF with posterior fixation	*Fusion rate (stand-alone ALIF): 51% *Fusion rate (ALIF with translaminar screw): 58% *Fusion rate (ALIF with unilateral pedicle screw): 89% *Fusion rate (ALIF with unilateral pedicle screw): 88%
Brantigan *et al.* (2004) [16]	To determine the long-term results of patients who received Brantigan I/F cage	10-year / PLIF with posterior fixation	*Patient satisfaction: 93.9% of 33 patients *ASD (sign): 61% of 31 patients *ASD (severe): 20%
Park *et al.* (2004) [3]	Review the articles related to adjacent segment degeneration (ASD) after lumbar or lumbosacral fusion	36-369 months / ALIF and PLIF with or without posterior fixation	*ASD (with pedicle screw fixation): 12.2% to 18.5% *ASD (with other forms of fixation or with no fixation): 5.2% to 5.6%

2.4. Non-fusion Spinal Techniques

In contrast to fusion surgery, the concept of non-fusion surgery is to restore normal physiological motions, or to allow restrained motions within a certain range, through various mobile non-fusion devices that aim to avoid or alleviate ASD disease. Currently, there are several types of non-fusion devices that have been developed worldwide, such as artificial discs, nucleus prostheses, total facet arthroplasty systems, pedicle-based dynamic stabilization systems, and interspinous process spacers [37]. In general, most non-fusion devices are designed to either reconstruct the posterior elements (facet joints, ligaments) or replace only the nucleus pulposus. An artificial disc is the only device that is designed to replace all components of a degenerative disc and restore normal physiological motions. Therefore, an artificial disc was chosen for evaluation in this study.

There is no difference between the approaches used for fusion and non-fusion surgeries. The choice of surgical approach depends on which type of non-fusion devices is used. Pedicle-based dynamic stabilization systems, interspinous process spacers, and total facet arthroplasty systems are used strictly for posterior approaches, while nucleus prostheses can be inserted using either an anterior or posterior approach. Due to the size of an artificial disc, only the anterior approach is used to insertion an artificial disc.

The standard artificial disc replacement surgical procedure includes removal of the ALL, the anterior portions of disc annulus, and the complete nucleus pulposus. However, surgeons can consider resuturing the ALL to increase stability and preventing implant dislocation.

2.4.1. Artificial Disc

The first artificial disc designed to restore the motion and function was introduced by Weber [38] in 1978. This type of artificial disc was designed to replace the degenerative disc and to restore a normal physiological ROM. In

general, there are some features that can be found in all lumbar artificial discs (Figure 2.12). First, the artificial disc is always composed of two or more components. In fact, the most popular design for artificial discs is a metal-polymer-metal sandwich structure, which includes metallic endplates and a relatively soft polymer core [39]. The metallic endplate can be attached into the vertebral body to form an articulated surface which to place the central core. The core can be put between the superior and inferior metallic endplates, thus providing various degrees of movement and weight bearing. Second, one or more gliding contact interfaces provide either the semi-constrained or unconstrained movements to facilitate spinal mobility. Third, some special designs and a bioactive porous coating are used on the contact surface of the metallic endplate facing the vertebral body. The metallic endplate designs have spikes or serrations that are perpendicular to the surface to allow for fixation to the vertebral body. The surface coating can encourage bony ingrowth along the adjacent vertebral body [40].

A number of lumbar artificial discs are currently either commercially available or under clinical trial, and the most popular designs are shown in Figure 2.12. These artificial discs can be classified by either the material used for gliding interface or the type of motion allow by the disc [41, 42]. The materials used for gliding interfaces include metal-polymer (Figure 2.12 (a) and (b)) or metal-metal (Figure 2.12 (c) and (d)), as listed in Table 2.2. The type of motion allowed varies widely depending on the design. Some allow unconstrained motion (Figure 2.12 (a) and (e)), and others allow only constrained or semi-constrained motion (Figure 2.12 (b), (c), and (d)).

The primary example of an unconstrained artificial disc is the mobile core configuration of the SB Charité III, which theoretically allows 5 degree of freedom (three unconstrained rotations and two unconstrained translations) and aims to restore nearly physiological center of rotation (COR) (Figure 2.13 (a)). In contrast, the primary example of a semi-constrained artificial disc is the

ball-and-socket configuration of the ProDisc II, which theoretically allows 3 degree of freedom (three unconstrained rotations and three constrained translations) and aims to reduce anteroposterior shear forces on the facet joint (Figure 2.13 (b)).

Galbusera *et al.* [41] reviewed 96 studies and reported on the biomechanics of unconstrained and semi-constrained designs for artificial discs in the lumbar spine. They found that both designs of artificial disc mentioned here seem to be able to restore nearly physiological COR locations and ROM values. Segment lordosis is increased after a lumbar total disc replacement in most cases, for both semi-constrained and unconstrained designs. In addition, most studies described an increase in facet loads, for both semi-constrained and unconstrained artificial discs, but with some contrasting results. Semi-constrained designs may be able to share a greater part of the load, thus avoiding overload of the surrounding soft structures, and the associated risks of possible early degeneration.

At present, both SB Charité III and ProDisc II designs are popular; however, ProDisc II is much cheaper than SB Charité III, which confers an economic advantage. Therefore, ProDisc II disc arthroplasty was selected to represent the non-fusion model in this study.

2.4.2. Clinical Outcomes Associated with Artificial Discs

In a series of clinical reports, the outcomes of patients treated with artificial discs were excellent; the range of patient satisfaction was between 72% and 98% (Table 2.3). Delamater *et al.* [43] reported that disc replacement patients had significantly less pain and disability at 6 weeks postoperatively compared with those undergoing a 360° lumbar fusion. At 6 months postoperatively, no significant difference was found in pain and functional outcomes for both groups, but motion was significantly improved in the disc replacement group. Zigler *et al.* [44] reported a 2-year follow-up of a prospective randomized FDA investigational study on the use of a ProDisc II device compared to a fusion

device. The intraoperation data indicated that disc replacement patients had shorter operative times, shorter hospital stays, and less intraoperative blood loss as compared with those undergoing lumbar fusion. At the 3-month follow-up, the disc replacement group had a significantly greater improvement in functional outcomes than did the fusion group. Bertagnolo and Kumar [45] described a study of 108 patients with different indications for total disc replacement at 3 months to 2 years of follow-up. Of these patients, 98.2% reported good and excellent results, with only one complication. However, progression of disc degeneration at adjacent levels was noted in 10 patients. Overall, the early clinical outcomes of artificial disc replacement are better than those associated with 360° lumbar fusion in patient satisfaction rate, intraoperative status, and functional outcomes. Only a few cases of ASD disease were noted.

Recently, several studies have reported mid-term and long-term clinical results of artificial disc replacement. Siept *et al.* [46] reported that multi-level disc replacement had a significantly higher complication rate and lower satisfaction rate at a 3-year follow-up. Less than 5% of patients had ASD or facet joint problems. Shim *et al.* [47] reported that clinical outcomes of both ProDisc and Charité groups were good at a 3-year follow-up, although unexpectedly high rates of facet joint degeneration at the surgical level and disc degeneration at the adjacent level were identified. Improvement rates and degeneration rates did not significantly differ between ProDisc and Charité. Marnay [48] indicated that 92.7% of patients were satisfied with the use of a ProDisc I artificial disc at 7-11 years long-term follow-up. Huang *et al.* [49] reported the results of an 8.7-year follow-up to evaluate the relationship between ROM and ASD disease after a lumbar total disc replacement. The overall prevalence of ASD was 24%, but was higher in patients with ROM of less than 5° (34%) (Figure 2.14). Although a high incidence of ASD was found, ASD had no statistically significant effect on clinical outcome. Guyer *et al.* [50] reported the only mid-term clinical results of artificial disc replacement versus anterior

fusion related to ASD disease. No statistical differences were found in clinical outcomes between disc replacement and fusion patients. However, fusion patients reached a statistically higher rate of long-term ASD disease, as compared with disc replacement patients.

In general, mid- or long-term follow-up studies show high patient satisfaction rates and good clinical outcomes associated with the use of either ProDisc or Charité artificial disc replacements [47-49, 46, 50]. Patient satisfaction rates may decrease due to multi-level disc replacement. In addition, a remarkably high incidence of ASD disease and facet joint degeneration at the surgical level were found in some reports [47, 49]; however, contrasting results were also reported [46, 48, 50]. Therefore, long-term complications of ASD and facet joint degeneration after using artificial discs remain unconfirmed, and require further research.

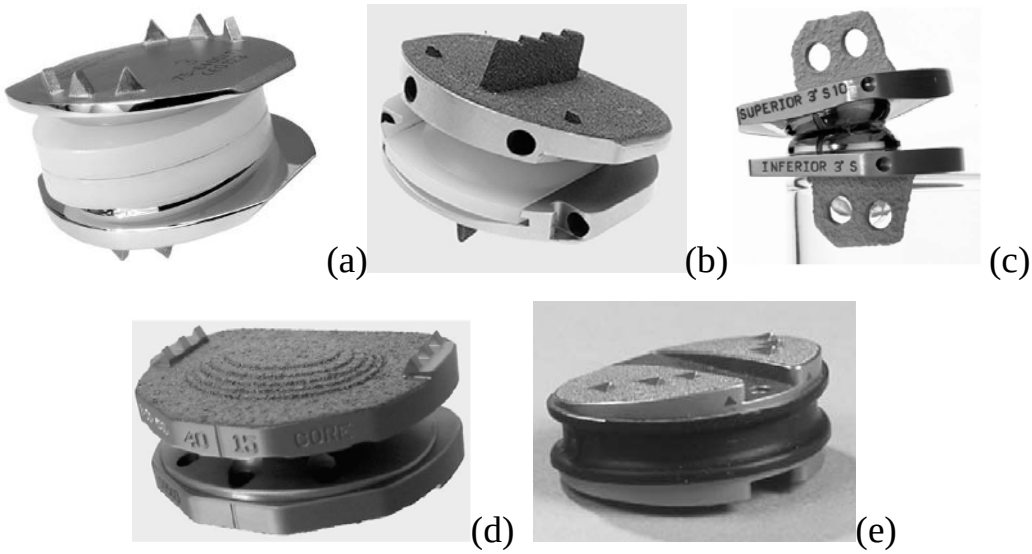

(a) (b) (c)

(d) (e)

Figure 2.12: Various lumbar artificial discs: (a) SB Charité III (Depuy Spine, Inc., Raynham, Massachusetts, USA); (b) ProDisc II (Synthes, Inc., Paoli, Pennsylvania, USA/ Spine Solution, New York, USA); (c) Maverick (Medtronic Sofamor-Danek, Inc., Memphis, Tennessee, USA); (d) FlexiCore (Stryker Spine, Allendale, New Jersey, USA/ SpineCore, Inc., Summit, New Jersey); (e) AcroFlex (Depuy Spine, Inc., Raynham, Massachusetts, USA).

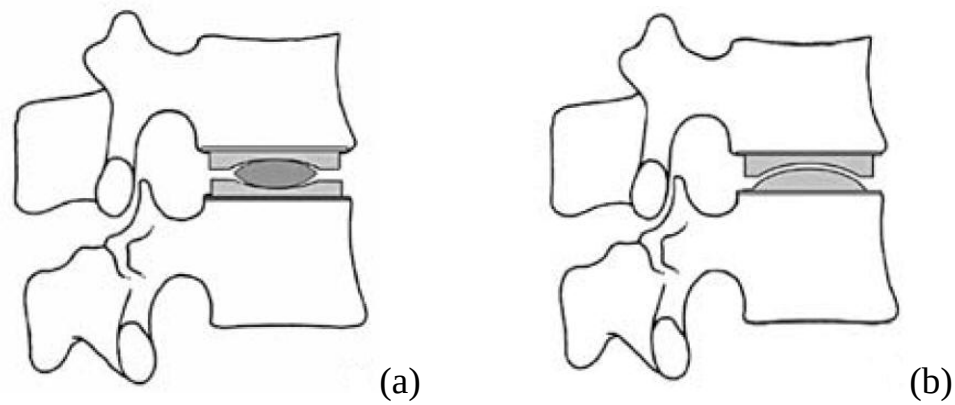

(a) (b)

Figure 2.13: Subcategories of artificial discs for motion include: (a) unconstrained design; (b) semi-constrained design [42].

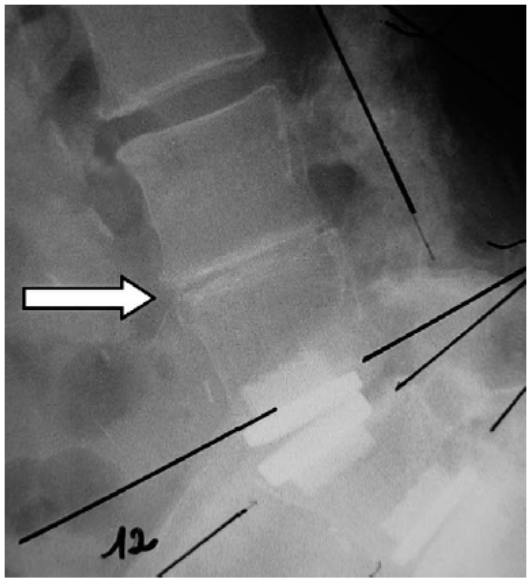

Figure 2.14: Adjacent segment degeneration after total disc replacement [49].

Table 2.2: Classification of lumbar artificial disc [51, 52]

Type	Material	Articulating Interface	Joint	Motion type	COR
SB Charité III	CoCrMo UHMWPE	Metal on Polymer	2	Unconstrained	Mobile
ProDisc II	CoCrMo UHMWPE	Metal on Polymer	1	Semi-constrained	Fixed
Maverick	CoCrMo	Metal on Metal	1	Semi-constrained	Fixed
FlexiCore	CoCrMo	Metal on Metal	1	Fully Constrained	Fixed
AcroFlex	Ti-6AL-4V Rubber	Metal bound rubber (Elastomeric)	-	Unconstrained	-

Table 2.3: Clinical outcomes of artificial disc

Authors	Purpose	Follow-up / Type of Artificial Disc	Outcome
Delamater *et al.* (2003) [43]	To evaluate early pain and functional outcomes of patients treated with disc replacement or fusion	6-month / ProDisc II	*Disc replacement patients reported earlier improvement in pain and function than did the fusion patients (6 weeks); however, there was non difference at 6 months.
Zigler (2003) [44]	To compare the disc replacement and lumbar fusion in a prospective randomized FDA investigational study.	2-year / ProDisc II	*Total disc replacement was associated with less blood loss, reduced operative time, and reduced length of hospital stay compared to combined with anterior-posterior lumbar fusion.
Bertagnolo and Kumar (2002) [45]	To find clinical outcome of patients treated with ProDisc II for various indications.	3-month to 2-year / ProDisc II	*Overall clinical outcome: 98.2% of 108 patients * ASD: 10 of 108 patients
Siept *et al.* (2006) [46]	Mid-term clinical results of total lumbar disc replacement for different indications.	3-year / ProDisc II	* Satisfaction rate: 82.6% of 92 patients *Satisfaction rate (one-level vs. two-level): 85.7% vs. 64.3% *ASD (Severe): 2.2% of 92 patients *Facet joint problems: 2.2% of 92 patients
Shim *et al.* (2007) [47]	To evaluate and compard clinicaland radiologic outcomes of the ProDisc and Charité.	3-year / ProDisc II or Charité III	*Clinical success rate (ProDisc vs. Charité): 83.3% (20 of 24 patients) vs. 93.9% (31 of 33 patients) *ASD (ProDisc vs. Charité): 28.6% (6 of 21 segments) vs. 19.4% (6 of 31 segments) *Facet joint degeneration at the surgical level (ProDisc vs. Charité): 32% (8 of 25 segments) vs. 36.4% (12 of 33 segments) *The degeneration rates of facet joints and disc at adjacent level between two groups were not significantly different.
Marnay *et al.* (2002) [48]	Long-term results of the ProDisc	7-11 years / ProDisc I	*Satisfaction rate: 92.7% of 55 patients. *There was no evidence of subsidence or migration.
Huang *et al.* (2006) [49]	To determine the relationship between range of motion (ROM) and adjacent segment degeneration (ASD)	8.7-year / ProDisc II	*ASD: 24% of 42 patients *Patients with motion less than 5° (29 patients) had a 34% prevalence of ASD. *ASD had no statistically significant effect on clinical outcome.
Guyer *et al.* (2009) [50]	To compare mid-term clinical results of lumbar disc replacement using Charité versus anterior lumbar interbody fusion using BAK cage.	5-years / Charité III	*Satisfaction rate (Charité vs. BAK): 78% (90 patients) vs. 72% (43 patients) *Disc height: similar for both groups *ASD (Charité vs. BAK): 8% (90 patients) vs. 20.9% (43 patients)

2.5. Development of Spinal Testing Protocols

Clinical reports have demonstrated long-term complications of ASD disease induced by spinal fusion surgery. The reasons for this disease may be explained by the concentration of stress and redistribution of motion along the spine after implanting various fusion devices. Therefore, many biomechanical studies have been undertaken to evaluate adjacent level effects (ALEs) of lumbar spines through ROM, intradiscal pressure, facet joint loading, or stress analysis to predict ASD disease in its early stages. However, conflicting results were found in these studies: increases in ALEs [53-59], no significant difference in ALEs [60-64], and decreases in ALEs [56, 57] have all been reported by several research groups. These inconsistent results may be due to differing testing protocols used to evaluate ALEs.

At present, several spinal testing protocols have been reported and used to predict ALEs, such as the LCM, the displacement control method (DCM), and a new HCM. However, it is still not clear which testing method is more suitable for revealing the physical effects of spinal implants. The following sections will introduce and review the results of these testing protocols in evaluating ALEs after simulating spinal fusion surgery.

2.5.1. Load Control Method

The load control testing method, also called the flexibility testing method, was proposed by Panjabi over three decades ago to be used for spinal testing [65]. This loading method applies the same pure moment to all spinal constructs, and then calculates the motions in each level. A pure moment is produced by applying two parallel forces, equal in magnitude, opposite in direction, and separated by a distance. The pure moment has two advantages. First, the pure moment applied to the end-vertebrae is applied equally to all the segments of the specimen. Second, the pure moment remains the same as the spine deforms during testing [66]. In general, the moment may range from 6 to 10 N-m for the

lumbar test [67]. In addition, a low compressive preload (100-200 N) was sometimes applied to the specimen in order to tighten and stabilize the spinal implant between two vertebrae.

Several biomechanical studies have attempted to evaluate ALEs after simulating lumbar spinal fusion by using the LCM [53-55, 60-64]. Cunningham *et al.* [53] compared the adjacent level kinematics of total disc arthroplasty versus conventional fusion fixation using five-level cadaveric lumbosacral spines. The results indicated that ALEs were markedly increased in both groups, including the BAK cage and the BAK cage combined with pedicle screws, under all physiological motions. Rao *et al.* [55] evaluated anterior cages in a calf lumbar spine model. The results showed that a small to moderate increase in motion was found at both adjacent levels in flexion and lateral bending. Intradiscal pressure changes at the inferior adjacent level were not significant. Sudo *et al.* [54] used ten calf spinal (L3-S1) specimens to evaluate five different lumbar reconstruction techniques on adjacent-level intradiscal pressure. They were unable to detect any difference in ALEs in their model of one-level posterior lumbar interbody fusion combined with pedicle screw fixation. However, a two-level fusion procedure significantly increased adjacent intradiscal pressure compared to the one-level fusion procedure. Rohlmann *et al.* [62] evaluated ALEs in ROM and intradiscal pressure at the levels above and below the internal fixator with use of the five-level cadaveric lumbosacral spines. The results indicated that using an internal fixation device on a spine specimen greatly affects intradiscal pressure changes and ROM at the surgical level. However, in most cases, ALEs in ROM and intradiscal pressure were small when load-controlled moments were applied. Similar results were also reported by Schmoelz [61, 64]. Rohlmann *et al.* [63] attempted to determine the influence of fixator stiffness on stresses in adjacent discs using FE analysis. Results showed that the maximum change of the von Mises stresses in the adjacent level discs was less than 10% when compared with the maximum value. Therefore,

they concluded that the stiffness of an internal spinal fixation device has only a minor influence on stresses in the adjacent discs.

In summary, the use of the LCM in evaluating stability of the whole lumbar spinal structure or the surgical level has been accepted, and stabilizing characteristics can be found [53-55, 60-64]. Although a number of studies revealed that the ALEs are greatly increased, or exhibit small to moderate increases with use of the LCM [53-55], most studies can not compute ALEs significantly when using only this testing protocol (Table 2.4).

2.5.2. Displacement Control Method

The displacement control testing method, also called the stiffness testing method, applies the same rotation-input to the spinal constructs, and then obtains the load-output behavior. There are several practical difficulties involved in using this method, especially for long spine with many segments [66, 68]. First, an axis of rotation must be defined before applying the rotation. However, the ideal location of the axis of rotation is not known prior to the first test, and different locations may be defined due to different experimental apparatus, manipulators, or specimens used. In addition, there is significant variability in the load-displacement curves, related to the location of the axis of rotation [69]. Therefore, the ideal axis of rotation is difficult to reproduce. Second, the ideal axis of rotation is cannot remain in the same location during the entire test, due to non-linear deformations of the spine. Third, if the axis of rotation is not in the ideal location, then spinal motions will be constrained, and can cause injury to the specimen. Fourth, the ideal axis of rotation will change after implanting various spinal implants. Beause of these disadvantages, the DCM is not often used to evaluate spine biomechanics like the LCM. In general, the rotation angle may range within physiological motion parameters, from 10° to 20° under flexion, and 5° to 15° under extension for the lumbar test (Table 2.5). Similar to the LCM, a 100~200 N compressive preload may be applied.

Several studies have used the DCM to evaluate ALEs after implanting various lumbar spinal fusion devices, and results are listed in Table 2.5 [56-59]. Shono *et al.* [57] used eighteen calf lumbosacral spine (L3-Sacrum) specimens to evaluate four posterior instrumentation systems in ROM changes at the both the surgical and adjacent levels. As segmental spinal instrumentation progresses from one level to three levels, the stiffness of the system significantly increases. However, ALEs were only detected at the upper level when using the Isola fixation system. In addition, ALEs decreased when using the Cotrel-Dubousset (CD) fixation system. Chow *et al.* [56] evaluated ALEs in ROM and intradiscal pressure at the levels above and below the fusion site with the use of six L1-S3 cadaveric lumbosacral spine specimens. The results indicated that fusion greatly affects ROM at both adjacent levels in flexion but not in extension. The intradiscal pressures of all unfused discs were only minorly increased in both flexion and extension, and the differences are within 5%. Cunninghum *et al.* [58] used 11 lumbosacral human cadaveric spinal specimens (T10-Sacrum) to evaluate changes in intradiscal pressures at adjacent levels under conditions of spinal reconstruction. In the instrumentation groups, disc pressure at the upper level increased by as much as 45%, whereas disc pressure at the surgical level decreased by between 41-55%.

In summary, stiffness of instrumentation can be evaluated in most biomechanical studies by using the DCM [56-58]. The DCM seems to be a better method for predicting ALEs due to the large increases of ROM and intradiscal pressure that were revealed, as compared with the LCM [56-59]. However, there is large variation in the reported ALEs, and results are conflicting between studies; increases in flexion [56-57, 59], increases in both flexion and extension [58], decreases in extension [56], decreases in both flexion and extension [57], and small changes [56] have all been independently reported (Table 2.5). Therefore, the DCM is not a proper method for revealing ALEs.

2.5.3. Hybrid Control Method

The HCM was first introduced by Panjabi in 2002 [70]. This approach applies different pure moments to each of the spinal constructs, and then the same overall ROMs are achieved for both intact and implant models. A detailed description of this method was presented in 2007 [66]. The four steps of the HCM are described in detail below.

(1) The specimen and its preparation: in order to reveal characteristics of motion redistribution, the whole mobile region should be tested. Therefore, the specimen of a T12-S1 long segment is recommended for *in vitro* testing.

(2) The intact spine test: the traditional LCM is used for testing the intact lumbar spine, and the specimens should not incur injury during the test. Then, the total ROM of the intact lumbar spine is measured.

(3) The spinal construct test: the spinal construct (specimen with a fusion and/or a non-fusion device) is subjected to increasing pure unstrained moments until the total ROM of the construct equals the ROM of the intact spine measured with the LCM (step 2).

(4) Data analysis: in order to evaluate ALEs, the increase in ROM or other biomechanical parameters at a non-operated spinal level is measured.

Goel *et al*. [71] indicated that, in real life, people bend their spines within a similar, limited ROM regardless of whether their spine is healthy or has undergone spinal surgery. In addition, the patient's main aim following surgery is to return to normal daily life. Thus, the surgically treated spine should be able to go through the same ROM as in a normal person. Therefore, they suggested that the spinal construct should be tested under the same ROM and the HCM should be more clinically relevant.

Currently, a number of studies have evaluated spinal implant biomechanics using the HCM [66, 71-73]. However, only one study has focused on the differences between the LCM and HCM. Goel *et al.* [71] analyzed ALEs of artificial discs that used both the LCM and the HCM, and revealed that ALEs

were not obvious under the LCM, while the ALEs (in this case, decreased ROM) were obvious under the HCM. It is still not clear whether the LCM or the HCM is more suitable to reveal the physical effects of spinal implants. Therefore, current study used FE analysis with both the LCM and HCM to explore biomechanical differences, at the implant level and at adjacent levels, between anterior fusion and non-fusion spinal implants.

Table 2.4: Adjacent level effects of lumbar spines were evaluated in flexion and extension under the load control method.

Author	Fusion level ; Fusion device	Increase in ROM normalized to intact (%)				Applied moment (Nm)
		Upper level		Lower level		
		Flexion	Extension	Flexion	Extension	
Cunningham *et al.* (2003) [53]	L4-L5 ; BAK+Isola fixation	11		20		8
Schmoelz *et al.* (2003) [64]	L3-L4 ; Fixator	NS	NS	NS	NS	10
Rao et al. (2006) [55]	L3-L4 ; LT-Cage	12.5	NS	11.3	NS	8.5
Rohlmann *et al.* (2001) [62]	L2-L4 ; Fixator	S	NS	S	NS	3.75
		Increase in intradiscal pressure normalized to intact (%)				
Schmoelz *et al.* (2006) [61]	L3-L4 ; Fixator	< 5 (NS)	< -10 (NS)	-	-	10
Rao *et al.* (2006) [55]	L3-L4 ; LT-Cage	21	-16 (NS)	10	-5 (NS)	8.5
Sudo *et al.* (2006) [54]	L5-S1 ; Brantigan cage+Isola fixation	80 (S)	60 (S)	-	-	6
Rohlmann *et al.* (2001) [62]	L2-L4 ; Fixator	NS	S	S	NS	3.75

Note: "NS" denotes not significant. "S" denotes significant.

Table 2.5: Adjacent level effects of lumbar spines were evaluated in flexion and extension under the displacement control method.

Author	Fusion level ; Fusion device	Increase in ROM normalized to intact (%)				Applied displacement (degrees)
		Upper level		Lower level		
		Flexion	Extension	Flexion	Extension	
Shono *et al.* (1998) [57]	L4/5 (one-level fusion)		20		-8	7.4 flexion 5 extension
	L4/L6 (two-level fusion) ; Isola fixation		35		-50	
	L4/5 (one-level fusion)		-48		-8	
	L4-L6 (two-level fusion) ; CD		-12		-42	
Chow *et al.* (1996) [56]	L4/5; Bone cement (ALIF)	240	-9	169	-25	15 flexion 10 extension
		Increase in intradiscal pressure normalized to intact (%)				
Chow *et al.* (1996) [56]	L4/5 ; Bone cement (ALIF)	5	5	4	2	15 flexion 10 extension
Cunningham *et al.* (1997) [58]	L3/4 ; Pedicle screw fixation	30	45	17.5	40	12.5 flexion 12.5 extension
	L3/L4 ; Isola fixation	25	35	10	35	
Weinhoffer *et al.* (1995) [59]	L5/S1 ; Pedicle screw fixation	30	-	-	-	20 flexion

2.6. *In Vitro* Test versus Finite Element Simulation

In vitro cadaveric tests and FE analyses are often used to assess the function of spinal implants, assess different surgical treatment scenarios, and predict short- or long-term pathological change before *in vivo* animal studies and clinical trials. The characteristics of *in vitro* tests are described below. First, the data are based on real test cases. Thus, the response of the neutral zone (the stiffness characterizing the lax deformation of the specimen) can be obtained. Second, the maximum failure load of the spinal construct can be obtained. However, there are some disadvantages. First, human cadaveric specimens are not easy to obtain in Taiwan. If animal specimens are used, the study is complicated by the large differences between humans and animals. Second, tests are time consuming and expensive. Third, large variances are found between specimens, which are related to age, aging, bone mineral density, or other factors. Fouth, it is not easy to overcome the drawbacks of measurement force and stress distribution on the soft tissue. Therefore, most *in vitro* studies still focus on the motion behavior of the lumbar spine.

There has been a rapid rise in the use of FE analysis to address the disadvantages of *in vitro* tests over the last decade [74-75]. FE analysis has several advantages. First, in an FE model, it is easy to modify geometry and material properties and assist in the design and development of the spinal implant. Second, stress distribution in each spinal structure can be revealed to understand how stress is redistributed after surgery. Third, it is easy to apply various testing protocols and loading cases to mimic different physiological conditions. The disadvantages of FE analysis are mentioned below. First, FE simulations will not indicate any unreasonable results. Therefore, engineers should independently judge the rationality of simulation results. Second, a convergence test and model validation must be executed before interpreting the data. However, it is difficult to validate a biomedical FE model due to the highly variable quality of cadaveric specimens. Therefore, discrepancies between *in*

vitro tests and FE simulations always exist. Third, it is not easy to obtain real material properties of spine. Lastly, there are some simplification and assumptions inherent in the FE model.

Chapter 3: Materials and Methods

The following sections include the FE modeling and simulation techniques used in this study. Three FE models of the lumbar spine were constructed for this study. The first model was of the intact lumbar spine. The other two models were of the lumbar spine implanted with: 1) a SynCage-Open plus bilateral pedicle screw fixation, and 2) a ProDisc II artificial disc. In addition, convergence tests of the intact lumbar spine model, as well as boundary and loading conditions of the LCM and HCM, are also described in the chapter.

3.1. FE Model of the Intact Lumbar Spine (INT model)

To create a three-dimensional FE model, computed tomography scan DICOM files of the L1 to L5 lumbar spine of a middle-aged male were obtained at 1-mm intervals. The commercially available visualization software Amira 3.1.1 (Mercury Computer Systems, Inc., Berlin, Germany) was used to describe cross-section contours of each spinal component in accordance with gray scale value (Figure 3.1). Then, the three-dimensional surface geometries were constructed through sequential processed cross-section contours as shown in Figure 3.2 (a). Each spinal component was exported as a Drawing eXchange Format (DXF) file and converted to the Initial Graphics Exchange Specification (IGES) file as shown in Figure 3.2 (b). The FE analysis software ANSYS 9.0 (ANSYS Inc., Canonsburg, PA) was used to reconstruct the FE model by converting the IGES file to ANSYS Parametric Design Language (APDL) code Figure 3.2 (c). The INT model was an osseo-ligamentous lumbar spine, which included the vertebrae, intervertebral discs, endplates, posterior bony elements, and all seven ligaments (Figure 3.3 (a)).

An eight-node solid element (SOLID185) was used for modeling the cortical bone, cancellous bone, posterior bony element, cartilage endplate, and

annulus ground substance. The cortical bone and cancellous bone were assumed to be homogeneous and transversely isotropic [76]. The posterior bony element and cartilage endplate were assumed to be homogeneous and isotropic [77]. The intervertebral disc consisted of annulus ground substance, nucleus pulposus and collagen fibers embedded in the ground substance. The nonlinear annulus ground substance was simulated by using a hyper-elastic Mooney-Rivlin formulation [78-79]. The collagen fibers simply connected between nodes on adjacent endplates to create an irregular criss-cross configuration. These irregular angles of collagen fibers were oriented within the range of the Marchand's [8] study. In the radial direction, twelve double cross-linked fiber layers were defined to decrease elastic strength proportionally from the outermost layer to the innermost. Therefore, the collagen fibers in different annulus layers were weighted (elastic modulus at the outermost layers 1-3: 1.0, layers 4-6: 0.9, layers 7-9: 0.75, and at the innermost layers 10-12: 0.65; cross sectional areas at the outermost layers 1-3: 1.0, layers 4-6: 0.78, layers 7-9: 0.62, and at the innermost layers 10-12: 0.47) based on previous studies [80-81]. The nucleus pulposus was modeled as an incompressible fluid with a bulk modulus of 1666.7 MPa by eight-node fluid elements (FLUID80) [77]. The 43% of the cross-sectional area in the disc was defined as the nucleus, which was within the range of the study by Panagiotacopulos (30-50%) [7]. Therefore, approximately 47% to 49% disc volume was assigned to nucleus pulposus. All seven ligaments and collagen fibers were simulated by two-node bilinear link elements (LINK10) with uniaxial tension resistance only, which were arranged in an anatomically correct direction [82]. The cross-sectional area of each ligament was obtained from previous studies [77, 81, 83-84], and material properties of the spine are listed in Table 3.1. The facet joint was treated as having sliding contact behavior using three-dimensional eight-node surface-to-surface contact elements (CONTA174), which may slide between three-dimensional target elements (TARGE170). The coefficient of friction was set at 0.1 [80]. The initial gap

between a pair of facet surfaces was kept within 0.5 mm as shown in Figure 3.3 (b) [77]. The stiffness of the spinal structure changes depending on the contact status, so the standard contact option in ANSYS was adopted to account for the changing-states nonlinear problem in this study. In addition, the element's shape will change after applying bending moments, thus changing the individual element stiffness. Therefore, the large displacement analysis option in ANSYS was chosen to solve this geometric nonlinear problem. The INT model consisted of 84,584 elements and 94,162 nodes.

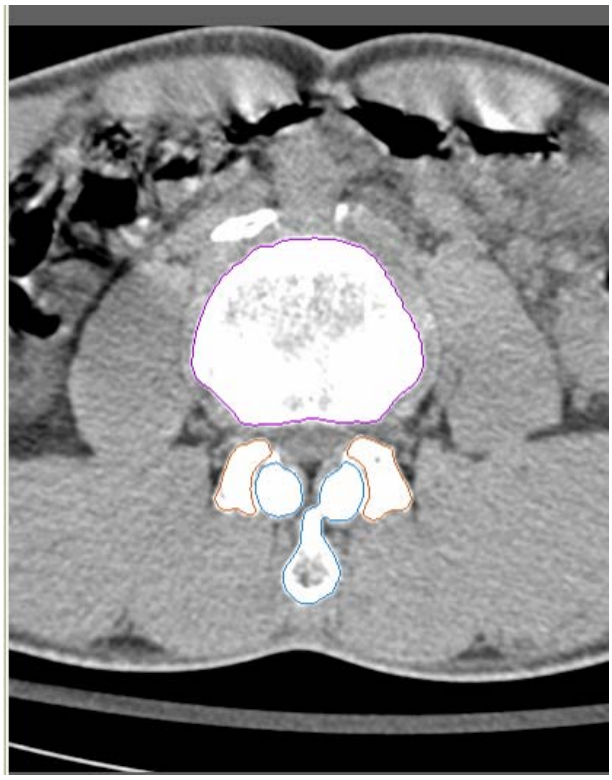

Figure 3.1: Each spinal component was selected from a computed tomography scan DICOM file to create material-related contours.

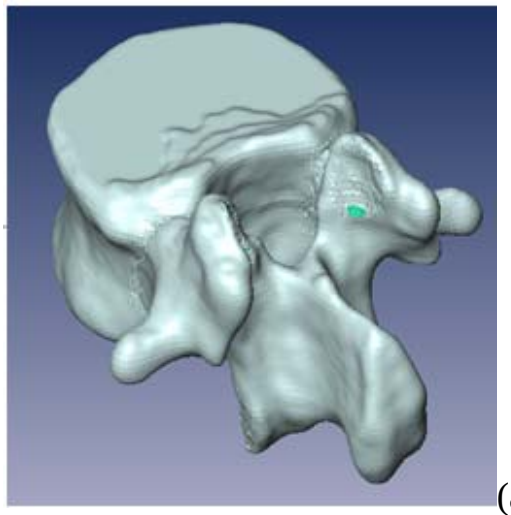

(a)

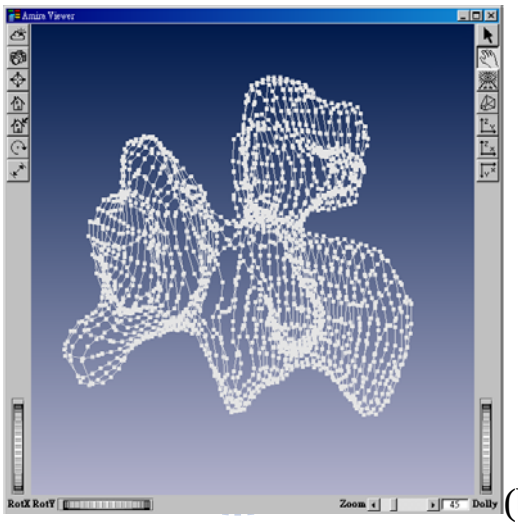

(b)

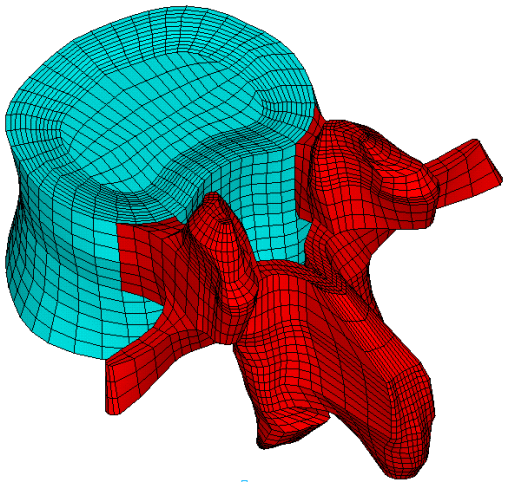

(c)

Figure 3.2: Modeling process of the L3 vertebra: (a) surface geometries of the L3 vertebra were reconstructed through sequential processed computed tomography scan DICOM files; (b) surface geometry was exported to the DXF file; (c) FE model of the L3 vertebra.

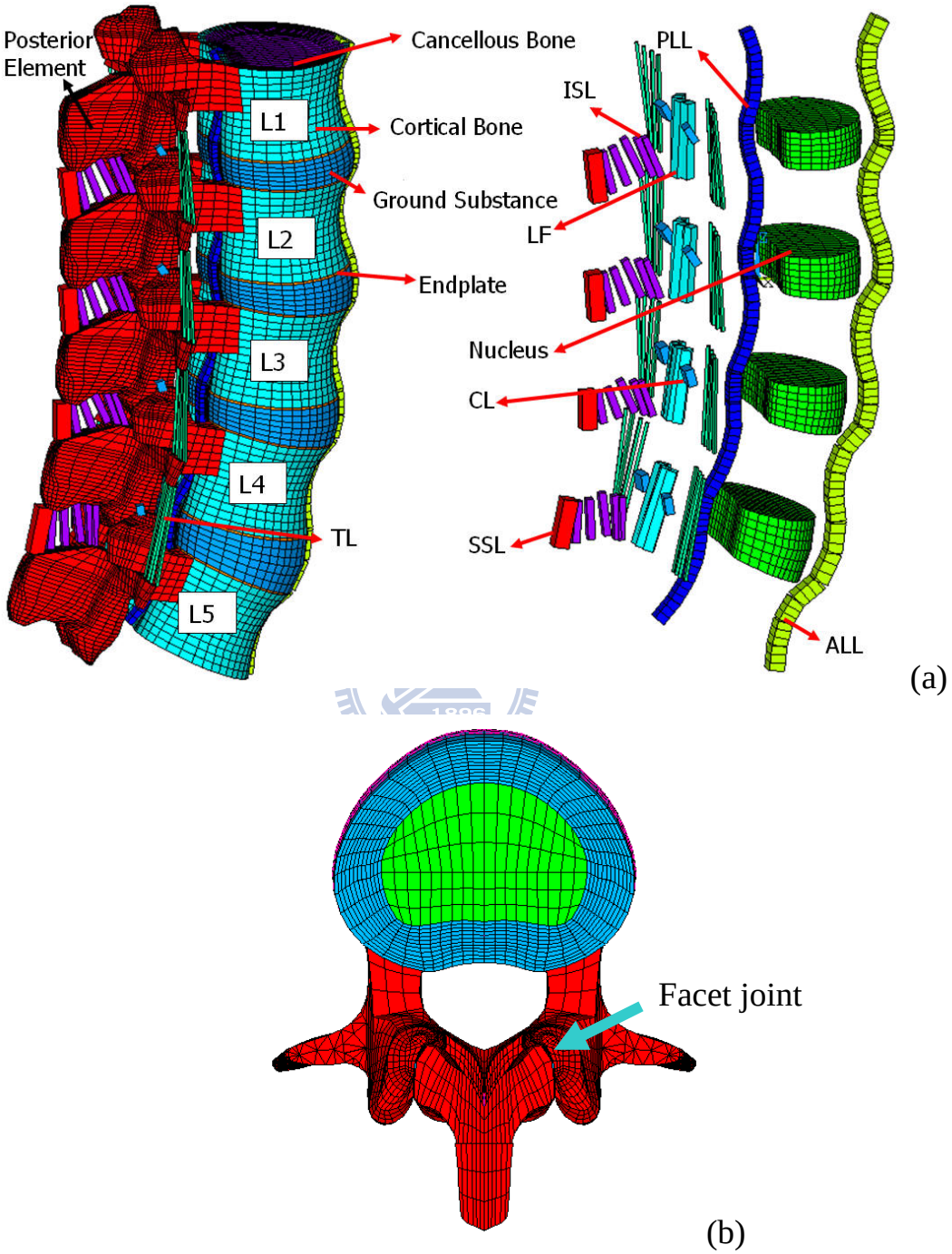

Figure 3.3: The finite element model of the L1 to L5 segments is shown: (a) intact model; (b) transverse views of facet joint curvature and gap.

Table 3.1: Material properties used in the FE model

Material	Element type	Young's modulus (MPa)	Poisson's ratio	Area (mm^2)	References
Vertebral		E_x=11300	ν_{xy}=0.484	-	[76]
Cortical	8node-Solid 185	E_y=11300 E_z=22000 G_x=3800 G_y=5400 G_z=5400	ν_{xz}=0.203 ν_{yz}=0.203		
Cancellous	8node-Solid 185	E_x=140 E_y=140 E_z=200 G_x=48.3 G_y=48.3 G_z=48.3	ν_{xy}=0.45 ν_{xz}=0.315 ν_{yz}=0.315	-	[76]
Posterior bony element	8node-Solid 185	3500	0.25	-	[77]
Disc					
Nucleus pulposus	8node-Fluid 80	1666.7	-	-	[77]
Ground substance	8node-Solid 185	C_{10}=0.42 C_{01}=0.105	-	-	[78, 79]
Annulus fibers	2node-Link 10				[80, 81]
Outmost (1-3 layers)		550	-	0.76	
Second (4-6)		495	-	0.5928	
Third (7-9)		412.5	-	0.4712	
Innermost (10-12)		357.5	-	0.3572	
Cartilaginous endplates	8node-Solid 185	24	0.4	-	[77]
Ligaments*	2node-Link 10				[77, 81, 83, 84]
ALL		7.8	-	24	
PLL		10	-	14.4	
TL		10	-	3.6	
LF		15	-	40	
ISL		10	-	26	
SSL		8	-	23	
CL		7.5	-	30	
Implants					
Spinal instrumentation (Titanium alloy)	2node-Beam 188	110000	0.28	D=6mm	
SynCage-Open (Titanium alloy)	8node-Solid 185	110000	0.28	-	
ProDisc metallic endplate (Co-Cr-Mo alloy)	8node-Solid 185	210000	0.3	-	
ProDisc inlay (UHMWPE)	8node-Solid 185	1016	0.46	-	[85]

*ALL, anterior longitudinal ligament; PLL, posterior longitudinal ligament; TL, transverse ligament; LF, ligamentum flavum; ISL, interspinous ligament; SSL, supraspinous ligament; CL, capsular ligament.

3.2. Convergence Test and Model Validation

In order to get reliable data, model validation and a convergence test were conducted. For the convergence test, three mesh densities (coarse model: 4,750 elements / 4,960 nodes; normal model: 27,244 elements / 30,630 nodes; finest model: 112,174 elements / 94,162 nodes) were selected to test for ROM changes in the INT model, and the finest mesh density was selected because the change were within 1.03% in flexion (less than 0.2^{o}), 4.39% in extension (less than 0.5^{o}), 0.01% in torsion (less than 0.2^{o}), and 0.001% in lateral bending (less than 0.1^{o}), respectively (Figure 3.4).

For the model validation, the loading condition was based on an *in vitro* study in which the multi-level lumbar spine was subjected to the maximum possible load without causing spinal injury [86]. Therefore, the LCM was used to validate all four physiological motions, i.e., flexion, extension, torsion, and lateral bending. Besides, facet contact force in torsion of each motion segment was compared with previous FE studies. In each case a moment of 10 N-m and a preload of 150 N were placed on the superior surface at the L1 level. In addition, the pure moments of 3.5 N-m and 7.5 N-m were also used in validating the INT model. These models constrained all degrees of freedom at the inferior surfaces of the L5 vertebra.

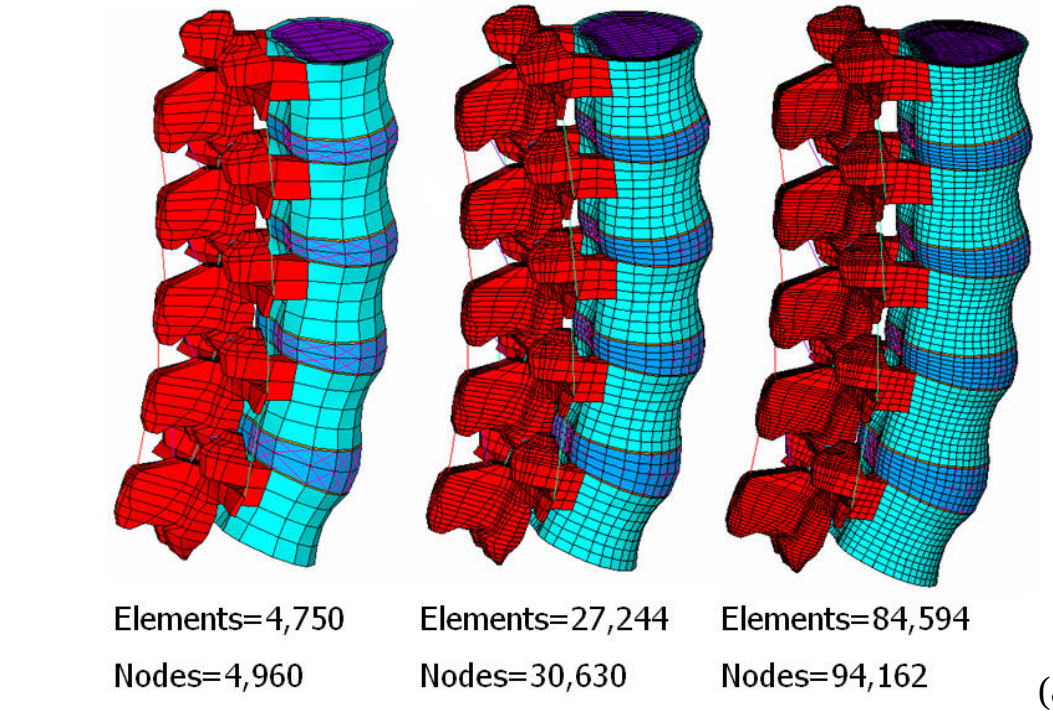

(a)

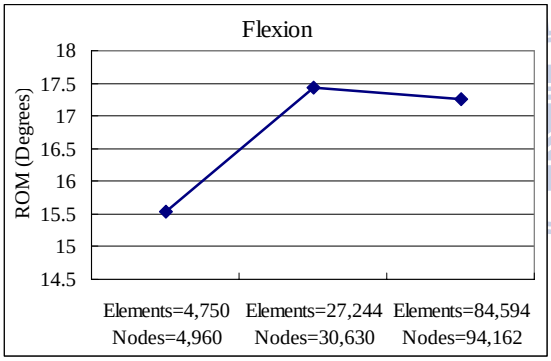

(b)

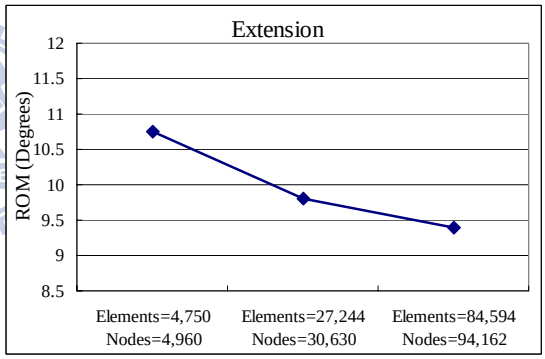

(c)

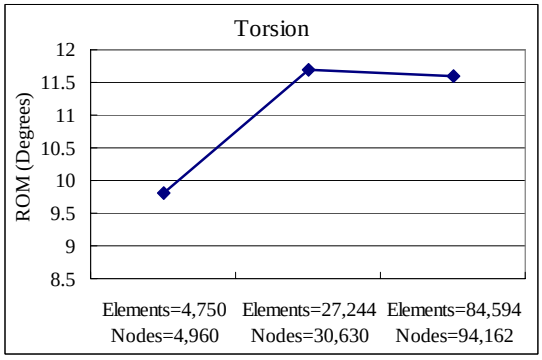

(d)

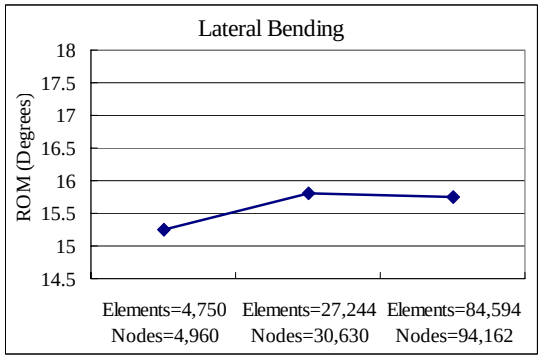

(e)

Figure 3.4: Convergence test of the intact model: (a) three mesh densities were selected for testing the range of motion; (b) result of motion changes under flexion; (c) result of motion changes under extension; (d) result of motion changes under torsion; (e) result of motion changes under lateral bending.

3.3. FE Model of the Anterior Lumbar Interbody Fusion (ALIF model)

To simulate the anterior lumbar interbody fusion, the L3/4 level of the INT model underwent partial discectomy and total nuclectomy by the anterior approach, which included removal of the anterior longitudinal ligament, anterior and some inner layer portions of the annulus, and the entire nucleus pulposus. All the other ligaments were preserved. Next, an 8° lordotic titanium alloy cage (SynCage-Open; 30 mm × 24 mm × 21 mm) supplemented with bilateral pedicle screw fixation was inserted. The material properties of the SynCage and posterior instrumentation system are listed in Table 3.1.

In this model, four pedicle screws (diameter, 6 mm) and two rods (diameter, 6 mm) were modeled with three-dimensional beam elements (BEAM188), then a full constraint behavior was designed between the screw-bone interface to simulate the pedicle screw bounded on the vertebrae. A SynCage was placed between the vertebral bodies, and the bone-cage interfaces were assigned fully bonded conditions to mimic a successful fusion. The ALIF model consisted of 139,692 elements and 99,924 nodes (Figure 3.5).

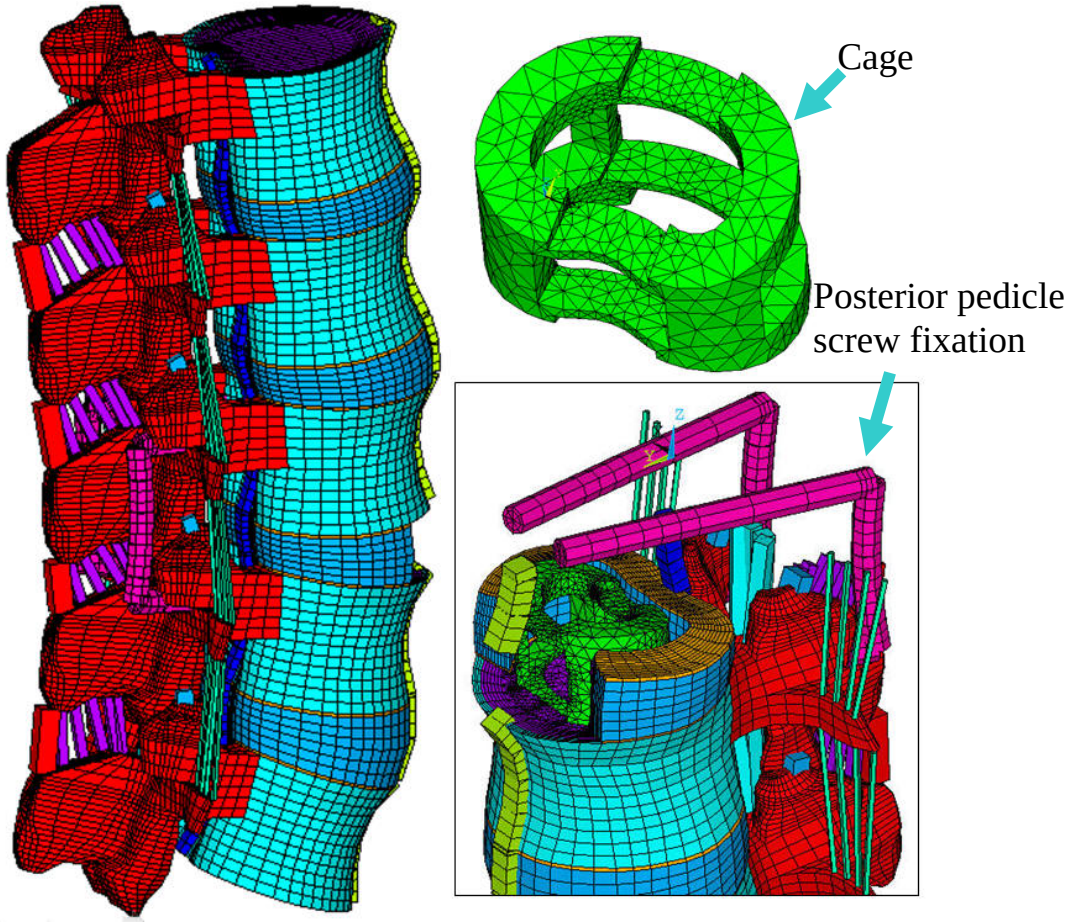

Figure 3.5: Finite element model of the anterior lumbar interbody fusion. The lumbar spine inserted in a SynCage-Open titanium interbody fusion cage supplemented with pedicle screw fixation at L3/L4 is shown.

3.4. FE Model of the Lumbar Artificial Disc Replacement (ADR model)

To simulate the total disc replacement, a ProDisc II was implanted into the INT model at L3/L4 following the standard total disc replacement procedure. The anterior and inner layer portions of annulus at L3/4 were removed. In addition, the nucleus of L3/4 was totally removed and all spinal ligaments were preserved. Figure 3.6 shows the remaining disc annulus and spinal ligaments after implanting ProDisc II. The material properties of the ProDisc II are listed in Table 3.1.

The keel of the metallic plate surfaces was modeled as a flat surface for simplification. A fully bonded condition was applied between the metallic plate and adjacent vertebrae to mimic a successful fusion. Deformable surface-to-surface contact behavior was used between the polyethylene inlay and the superior metallic plate, and the coefficient of friction for the polyethylene-CoCrMo alloy contact surface was chosen to be 0.07 [87]. The ADR model consisted of 113,315 elements and 91,126 nodes (Figure 3.6).

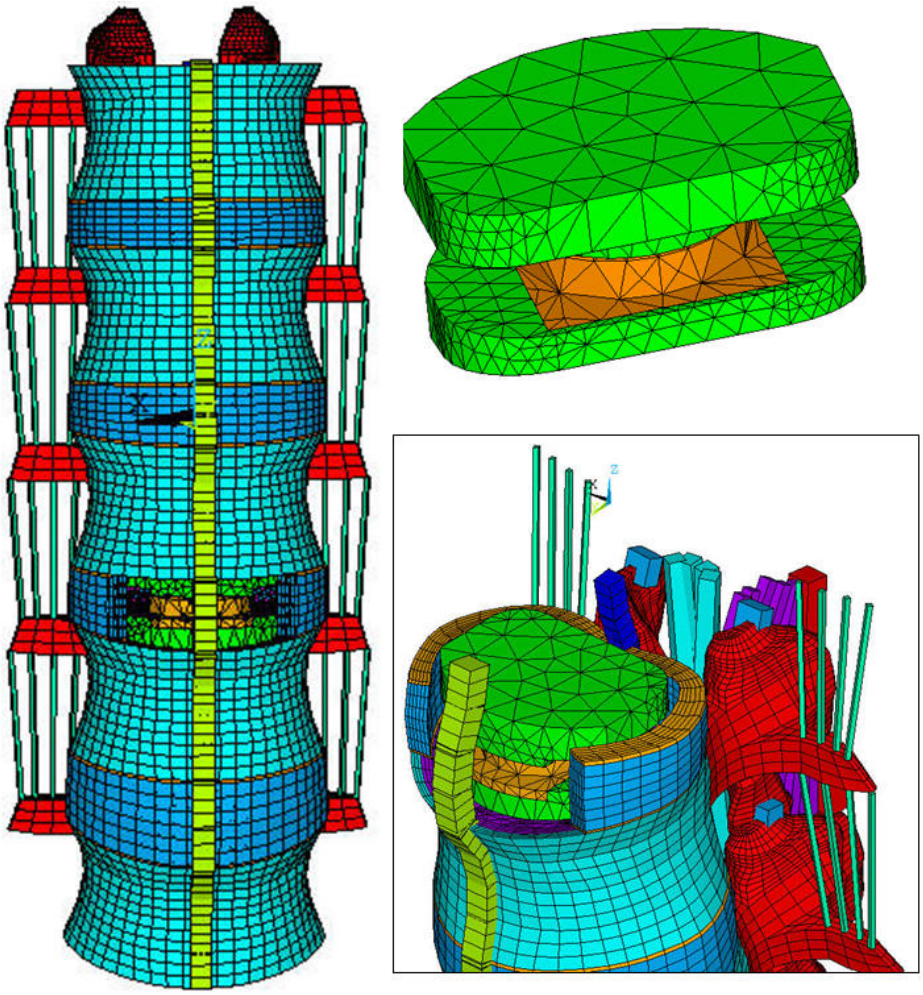

Figure 3.6: Finite element model of total disc replacement. The lumbar spine implanted with a ProDisc II artificial disc at L3-L4 is shown.

3.5. Boundary and Loading Conditions

The LCM and HCM were used to explore the differences at the implant and the adjacent levels. The LCM was the same control method that had been used in the model validation (10 N-m with 150 N preload). For the HCM, a 150 N preload was applied on the superior surface of the L1 vertebra, and then a higher pure moment of 30 N-m was applied incrementally by 0.3 N-m in 100 loading steps. The result of every substeps was saved. Therefore, the resultant ROMs (L1 to L5) of the ALIF and ADR models under different moments would match the ROMs of the INT model by using the LCM. The detailed total lumbar ROMs of the INT model under the LCM are 16.84^{o} in flexion, 14.73^{o} in extension, 9.48^{o} in torsion, and 17.14^{o} in lateral bending, respectively (Table 3.2). These ROMs are a baseline to match the total lumbar motion among the INT and surgical models under the HCM (Table 3.3). The resulting deviation of ROMs among the three FE models were controlled within 0.1^{o} in flexion, 0.13^{o} in extension, 0.05^{o} in torsion, and 0.08^{o} in lateral bending, respectively. The above hybrid control procedure used in this study was presented in detail in chapter 2.5. With both control methods, all the models were constrained at the bottom of the fifth vertebra.

Table 3.2: Intervertebral range of motion and applied moment among the INT, ALIF, and ADR models under the load control method.

Motion	Model	ROM (deg)				Total lumbar ROM (deg) (L1-L5)	Moment (N-m)
		L1-L2	L2-L3	L3-L4	L4-L5		
Flexion							
	INT	3.76	3.93	4.00	5.15	16.84	10
	ALIF	4.01	4.21	0.09	6.04	14.35	10
	ADR	3.76	3.86	4.37	5.23	17.22	10
Extension							
	INT	3.30	3.37	3.70	4.36	14.73	10
	ALIF	3.14	3.03	0.42	4.06	10.65	10
	ADR	3.69	3.54	6.69	4.37	18.29	10
Torsion							
	INT	2.03	2.16	2.50	2.79	9.48	10
	ALIF	2.05	2.05	1.07	2.72	7.89	10
	ADR	2.09	2.09	4.19	2.73	11.10	10
Lateral bending							
	INT	3.97	4.05	4.25	4.87	17.14	10
	ALIF	4.13	4.24	1.15	5.28	14.80	10
	ADR	3.80	3.80	6.14	4.66	18.40	10

Table 3.3: Intervertebral range of motion and applied moment among the INT, ALIF, and ADR models under the hybrid control method.

Motion	Model	ROM (deg)				Total lumbar ROM (deg) (L1-L5)	Moment (N-m)
		L1-L2	L2-L3	L3-L4	L4-L5		
Flexion							
	INT	3.76	3.93	4.00	5.15	16.84	10
	ALIF	4.69	4.92	0.65	6.55	16.81	12.9
	ADR	3.65	3.76	4.25	5.08	16.74	9.6
Extension							
	INT	3.30	3.37	3.70	4.36	14.73	10
	ALIF	4.38	4.24	0.65	5.55	14.82	16.2
	ADR	2.95	2.91	5.36	3.64	14.86	6.9
Torsion							
	INT	2.03	2.16	2.50	2.79	9.48	10
	ALIF	2.46	2.46	1.31	3.20	9.43	13.2
	ADR	1.72	1.85	3.56	2.37	9.50	7.8
Lateral bending							
	INT	3.97	4.05	4.25	4.87	17.14	10
	ALIF	4.89	4.92	1.31	6.02	17.14	12.3
	ADR	3.26	3.57	5.82	4.41	17.06	9

Chapter 4: Results and Discussion

The following section includes five parts. First, an intact spine model is validated through comparison of ROM to previous *in vitro* tests. Second, changes in ROM at the implant and adjacent levels on the ALIF and ADR models are compared to those of the intact lumbar spine under both the LCM and HCM. In addition, the trend of ROM changes in these cases is compared with previous biomechanical studies to validate both surgery models and find differences between them. Third, changes in facet contact forces (FCF) under extension and torsion are shown. In this part, the present study tries to explain the clinical findings of facet joint degeneration for both surgical techniques through this biomechanical parameter. Fourth, the stress distribution patterns in the adjacent L2/3 disc annulus are revealed under both loading conditions. Also, the present study tries to explain the possibility of accelerative disc degeneration at adjacent levels through annulus stress distribution patterns. And fifth, the limitations of this study are presented. In this study, all data were normalized to the INT model as percentage values under each loading mode.

4.1. Model Validation

The ROMs in five levels of the INT model under different loading moments were validated with previous *in vitro* cadaveric tests and analytical studies [86, 88-90] (Figure 4.1). Under a 10N-m moment with a 150 N preload, the current INT model showed some stiffer behavior in flexion and exhibited a 6° to 11° lower ROM value than the *in vitro* studies by Yamamoto *et al.* and Panjabi *et al.*, as shown in Figure 4.1(a) [86, 89]. In torsion, the difference between the INT model and the *in vitro* tests was less than 2°. Under 3.75 N-m and 7.5 N-m pure moments, all five levels of lumbar ROMs were within the range of extreme values in flexion-extension, right-left torsion, and right-left lateral bending, as compared to the results of the *in vitro* test without a follower load made by

Rohlmann *et al.* (Figure 4.1(b)) [90]. Overall, the trend of our FE simulation is closer to Rohlmann's study than Panjabi's and Yamamoto's *in vitro* studies. In addition, facet contact forces in left torsion of each motion segment were compared with Chen's [88] and Shirazi-Adl's [91] FE studies, which confirmed the values from the present FE model (Table 4.1).

The ROM of the present intact FE model is in good agreement with *in vitro* tests in terms of extension, torsion, and lateral bending [86, 89], whereas the ROM is 6° to 11° lower than that from the *in vitro* test under flexion. Eberlein *et al.* [92] also indicated that numerical results exhibited stiffer responses than the experimental results in terms of flexion. Their study indicated that these deviations can be reduced by assuming tissue degeneration in the annulus fibrosus and a complete loss of intradiscal pressure in the intervertebral discs. Therefore, they demonstrated that tissue degeneration plays an important role in the motion behavior of the lumbar spine. In the *in vitro* test performed by Rohlmann *et al.* [90], the older cadaver specimens revealed a larger variance in ROMs than younger specimens. This discrepancy may be the result of various stages of disc degeneration, such as microfissures in the disc, annulus bulging, damage to the endplate, or dehydration of the disc. Furthermore, specimens could possibly have suffered soft-tissue decay after a longer experimental time, and this may have caused extreme changes in stiffness in the specimens. Therefore, the fact that cadaveric specimens from the *in vitro* tests exhibited lower stiffness than the FE spine model analysis in flexion might be explained by tissue degeneration associated with the older cadaveric specimens that were used in the *in vitro* tests.

Although a discrepancy in flexion was noticed, ROMs and FCFs of the present intact FE model are close to values from Rohlmann's study and previous FE studies, respectively. Thus, this INT model was validated for further simulation analysis.

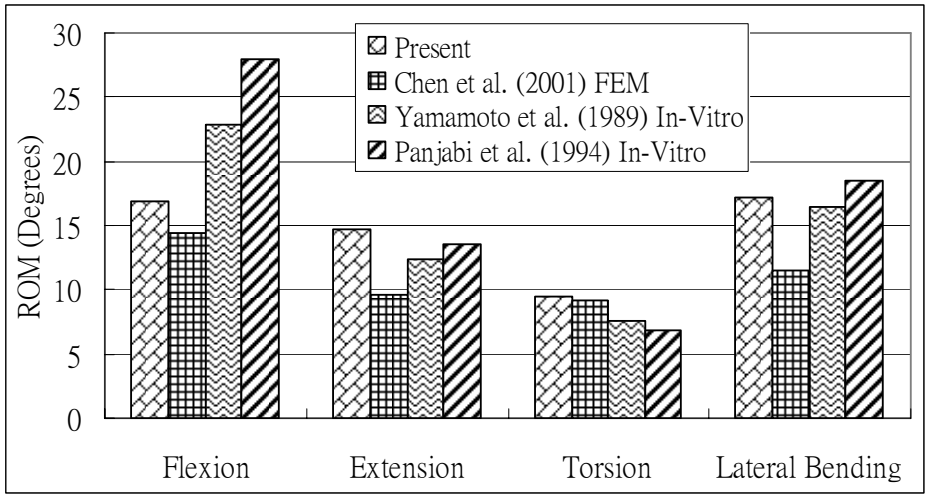

(a)

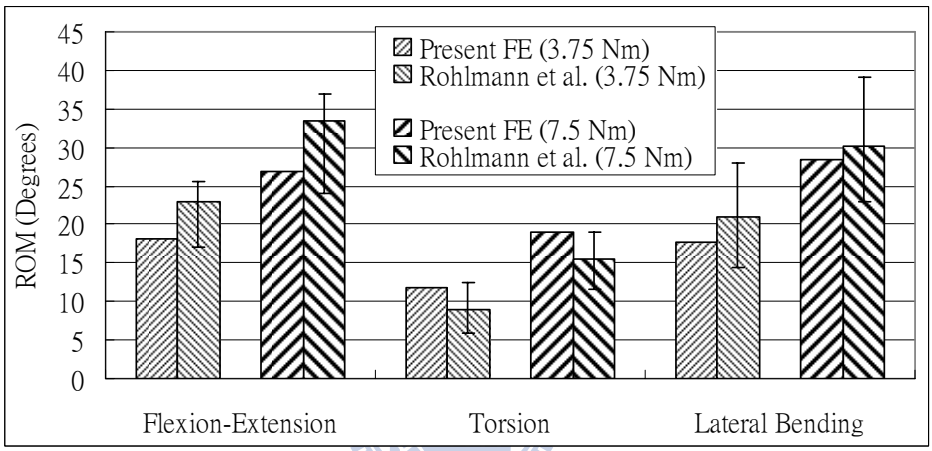

(b)

Figure 4.1: Comparison of ROM calculated for the five levels of intact lumbar spine with previous *in vitro* experiments and analytical studies: (a) loading of 10 N-m moments with 150 N preload in the present INT model; (b) loading of 3.75 N-m and 7.5 N-m pure moments in the present INT model. (The data in (b) include both side motions. Median and extreme values for the *in vitro* data are shown).

Table 4.1: Comparison of facet contact forces under torsion between the present study and studies by Chen and Shirazi-Adl. Unit: N

Left torsion	Loading conditions	L1-L2	L2-L3	L3-L4	L4-L5
Present study	10 N-m with 150 N preload	121	130	125	127
Chen's study [88]	10 N-m with 150 N preload	121	157	161	155
Shirazi-Adl's study [91]	10 N-m	107	123	117	78

4.2. Range of Motion

Implant Level Effects

Under the LCM, the ALIF model showed relative stability, compared with the INT model; the ROM was reduced obviously in flexion (-97.7 %), extension (-88.6 %), and lateral bending (-72.9 %), but less in torsion (-57.0 %), compared with the INT model. In contrast, the ADR model had a large ROM increase in extension (+81.1 %) (Figures 4.3(a)), torsion (+67.9 %) (Figure 4.4(a)), and lateral bending (+44.5 %) (Figure 4.5(a)), but less in flexion (+9.2 %) (Figures 4.2(a)). The ROM values of the LCM are listed in Table 3.2.

Under the HCM, the ROM of the ALIF model was reduced obviously in flexion (-83.7 %), extension (-82.4 %), and lateral bending (-69.2 %), but less in torsion (-47.6 %), compared with the INT model. In contrast, the ADR model had a large ROM increase in extension (+45.1 %) (Figures 4.3(b)), torsion (+42.7 %) (Figure 4.4(b)), and lateral bending (+37.1 %) (Figure 4.5(b)), but less in flexion (+6.4 %) (Figures 4.2(b)). The ROM values of the HCM are listed in Table 3.3.

Overall, both control methods can provide similar stability in the ALIF model. However, in the ADR model, the LCM showed prominently higher ROM increase than the HCM, especially in extension and torsion.

Comparison of the implant level effect between present FE models and previous studies under the HCM are listed in Table 4.1. For the implant level, the ALIF model showed similar stability with both control methods. Oxland and Lund indicated that anterior fusion plus posterior pedicle screw fixation can improve stabilization in all motions [93]. Gerber *et al.* [94] indicated that anterior cage plus posterior pedicle screw fixation did not provide significant stability in torsion with the LCM. This behavior of the LCM is similar to the *in vitro* test of Panjabi *et al.* [95] using the HCM, in which the ROM decreased by 77.4 % in flexion-extension, by 36.4 % in torsion and by 65.7 % in lateral bending. The results of our ALIF model are in agreement with most of the *in*

vitro test results [93-96], in that the fusion level can provide good stability in flexion, extension, and lateral bending, but is not so in torsion, regardless of whether the LCM or HCM is used.

The implant level of the ADR model shows significantly increased ROM in extension, torsion, and lateral bending under both control methods. In addition, the LCM showed higher ROM than the HCM, especially in extension and torsion. These characteristics of the ADR model are in agreement with a previous report by Goel *et al.* [71].

Therefore, this study suggests that both control methods can be adopted to evaluate the implant level of the fusion model, and similar stabilizing characteristics can be expected to be found. On the other hand, the effects on the implant level of the ADR increased ROM with the LCM, especially in extension (81.1 % vs. 45.1 %) and torsion (67.9 % vs. 42.7 %). Thus, LCM analysis might indicate a higher risk for patients with ADR implants. The present study suggests that the LCM might emphasize the effect on the implant level of the non-fusion model.

Adjacent level effects (ALEs)

The ALE% of the ROM was defined as the averaged percentage changes of the ROM from whole non-operated levels. Under the LCM, the ALE% of the ALIF model in flexion (+10.3 %) and extension (-7.3 %) were small, and in torsion and lateral bending were even smaller (average within 6 %). The ALE% values of the ADR model were close to those of the INT model in flexion (Figures 4.2(a)), extension (Figures 4.3(a)), torsion (Figures 4.4(a)), and lateral bending (average within 6 %) (Figures 4.5(a)).

Under the HCM, the ALE% of the ALIF model increased in flexion (+25.6 %), extension (+28.6 %), torsion (+16.7 %), and lateral bending (+22.8 %), as compared with the INT model. In contrast, the ALE% of the ADR model decreased obviously in extension (-13.6 %) (Figures 4.3(b)), torsion (-14.9 %)

(Figures 4.4(b)), and lateral bending (-13.0 %) (Figures 4.5(b)), but less in flexion (-2.9 %) (Figures 4.2(b)), as compared with those with the INT model.

The HCM increased the ALE% in ROM more than when using the LCM in the ALIF model; on the other hand, the HCM decreased the ALE% more than when using the LCM in the ADR model, especially in extension, torsion, and lateral bending.

The ALEs between present FE models and previous studies under the HCM are listed in Table 4.1. For the adjacent levels, the ALIF model shows a significantly increased ALE%, using the HCM. As mentioned previously, conflicting ALE% results were found with the LCM. The ALE% of the HCM determined in the current study are in the range of the values reported in the literature [73, 95-96], which showed significantly increased ALE% (Table 4.1). However, a few inconsistencies in ALE% were still noticed. In lateral bending, significantly increased ALE% with fusion was reported (average, +20.7 %) [73]; in contrast, a small ALE% with fusion was also found (average, +4.1 %) [95]. This discrepancy was also revealed in torsion [73, 95-96]. These different results might be explained that different fusion techniques were simulated between their studies. Despite these differences in ALEs, this study has shown that the HCM could emphasize the ALEs more than the LCM on the fusion model.

The ALE% of the ADR model was close to the INT model with the LCM, while it was significantly decreased with the HCM. This trend of an ALE% decrease was also found in other studies using the HCM [71, 95-96].

Overall, this study suggests that the HCM should be more effective in evaluating the ALEs of the fusion model. On the other hand, the HCM may decrease ALEs of the ADR. Verification of the influence of these abnormal motions requires more evidence through clinical research. Therefore, the present study suggests that both control methods should be used in evaluating ALEs of non-fusion models.

Clinical relevance of loading condition

Goel *et al.* [71] proposed that the patient's main aim following surgery is to return to normal daily life. Thus, the surgically treated spine should be able to go through the same ROM as in a normal person. However, in real life, people sustain the same external moments during lifting activities whether or not they have had surgery, making the LCM useful for evaluating this condition. The present study suggests that these two analytical methods could be used to predict specific conditions in the patient's daily life. The HCM is suitable for evaluating the patient's daily life motion during restoration after surgery, while the LCM is suitable for evaluating the patient's normal lift work-loading condition after surgery [97].

In summary, the present study indicates the difference in ROM changes between the LCM and HCM after using a fusion or non-fusion implant. Similar trends were found in present FE simulations of fusion or non-fusion implants compared to previous studies. In a way, these data validate the predictions of the ALIF and the ADR FE models. In addition, the present study suggests that these two analytical methods could be used to predict specific conditions in the patient's daily life.

Table 4.2: The implant and adjacent level effects on the lumbar spine after implantation of an anterior cage or an artificial disc were compared with previous finite element and *in vitro* studies under the hybrid control method.

Authors	Fusion or non-fusion implants	Increase in ROM normalized to intact (%)				Surgical level
		Implant level effect				
		Flexion	Extension	Torsion	Lateral Bneding	
Present FE model	SynCage plus pedicle screw fixation	-83.7	-82.4	-47.6	-69.2	L3-L4
	ProDisc*	+6.4	+45.1	+42.7	+37.1	
Goel *et al.* (2005) [71]	Charité*	+18.9	+43.3	-	-	L5-S1
Panjabi *et al.* (2007) [95]	Pedicle screw fixation	-77.4		-34.6	-67.5	L5-S1
	ProDisc*	-1.1		+72.8	+55.5	
Panjabi *et al.* (2007) [96]	Pedicle screw fixation	-81.1		-33.7	-	L5-S1
	Charité*	-2.7		+24.6	-	
Panjabi *et al.* (2007) [73]	Anterior plate plus pedicle screw fixation	-75.9		-65.5	-88.2	L4-L5
	StabilimaxNZ*	-34.5		+18.4	-36.1	
		Non-operated adjacent levels effect (ALE%)				
Present FE model	SynCage plus pedicle screw fixation	+25.6	+28.6	+16.7	+22.8	L3-L4
	ProDisc*	-2.9	-13.6	-14.9	-13.0	
Goel *et al.* (2005) [71]	Charité*	-9.5	-26.3	-	-	L5-S1
Panjabi *et al.* (2007) [95]	Pedicle screw fixation	+13.2		+5.98	+4.1	L5-S1
	ProDisc*	+1.4		-8.68	-4.1	
Panjabi *et al.* (2007) [96]	Pedicle screw fixation	+21.06		+5.64	-	L5-S1
	Charité*	+0.7		-4.6	-	
Panjabi *et al.* (2007) [73]	Anterior plate plus pedicle screw fixation	+17.7		+25.0	+20.7	L4-L5
	StabilimaxNZ*	+9.3		+0.2	+8.7	

Note: An asterisk (*) denotes the non-fusion spinal implant model.

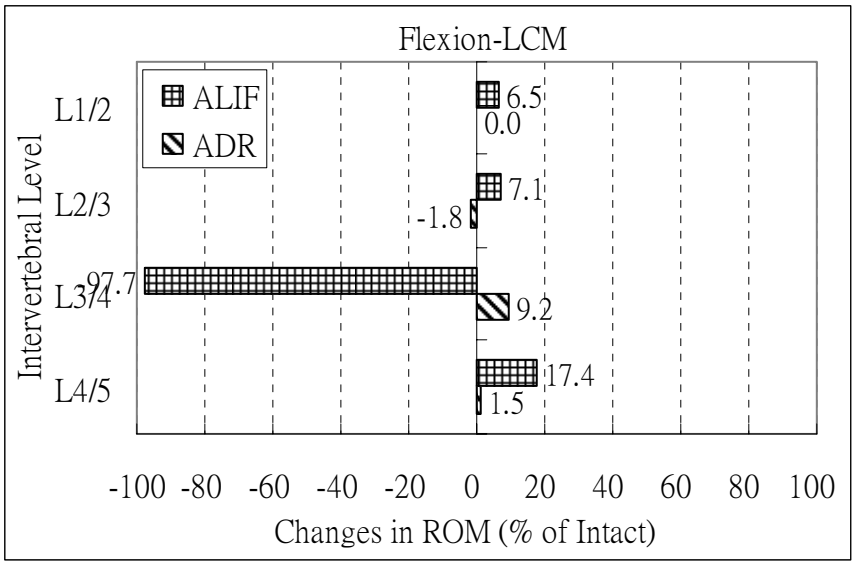

(a)

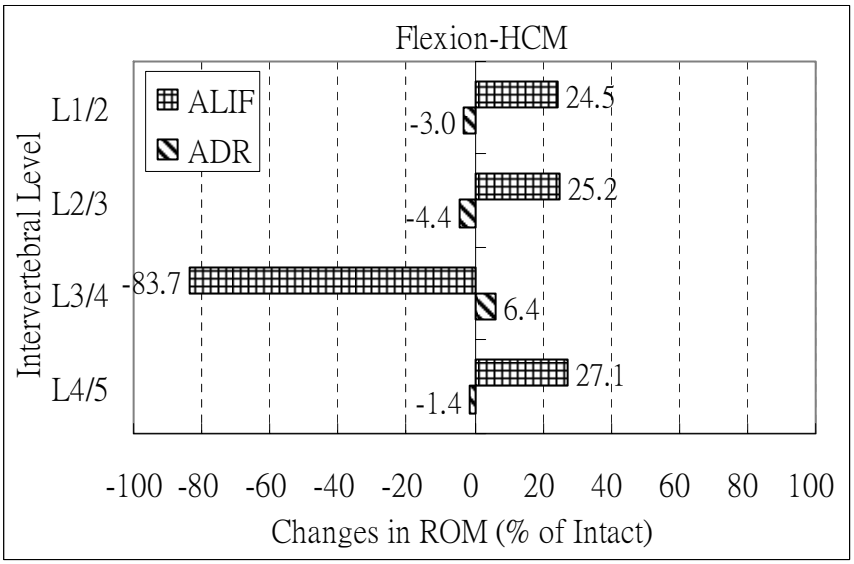

(b)

Figure 4.2: Changes in the ROM under flexion: (a) LCM results; (b) HCM results.

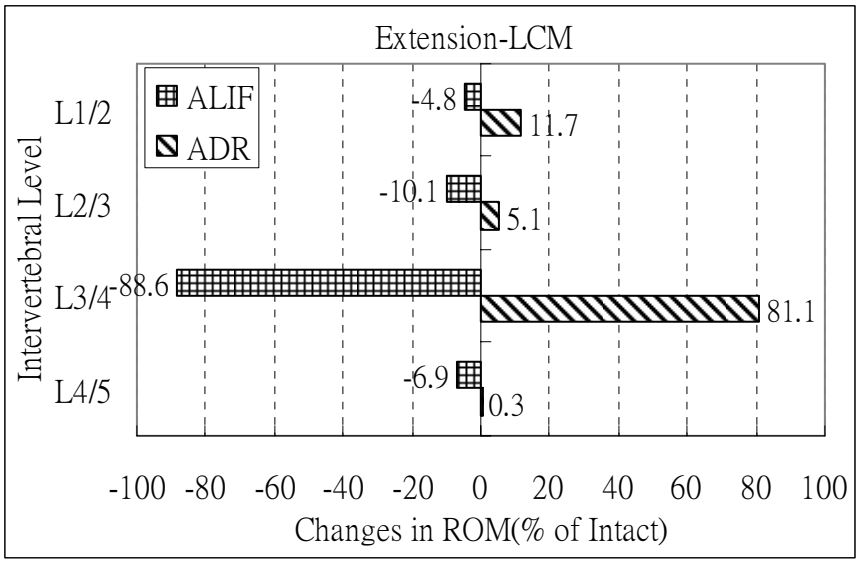

(a)

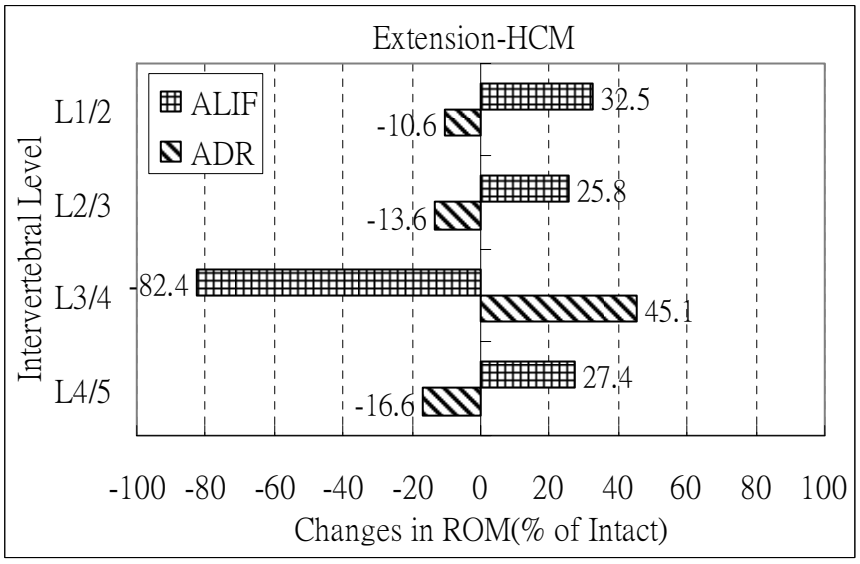

(b)

Figure 4.3: Changes in the ROM under extension: (a) LCM results; (b) HCM results.

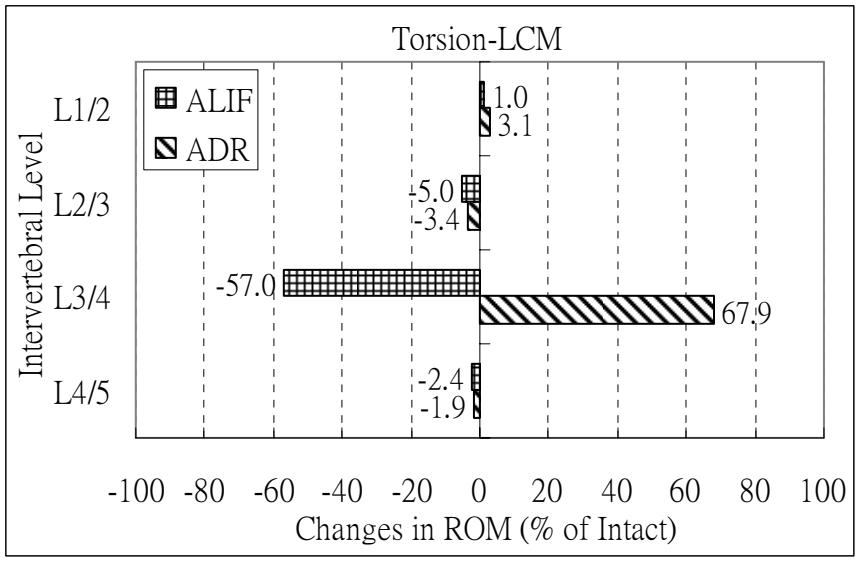

(a)

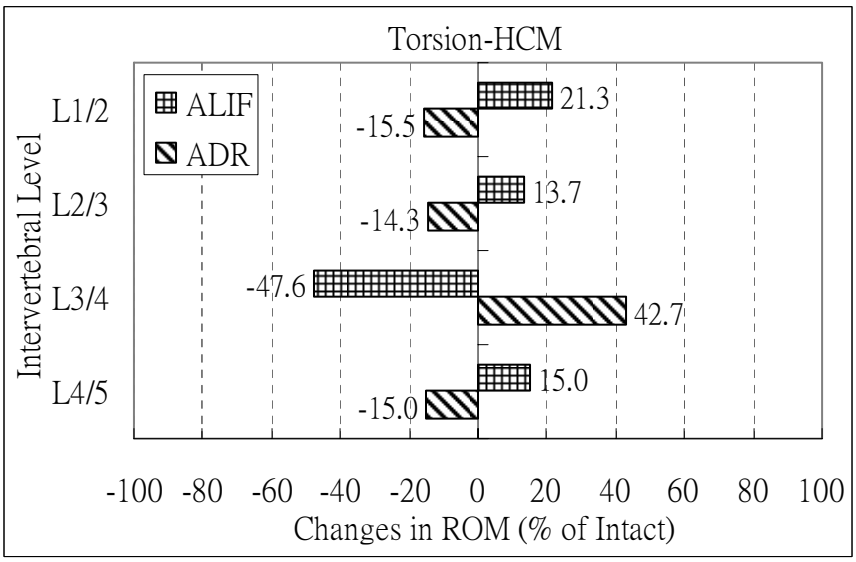

(b)

Figure 4.4: Changes in the ROM under torsion: (a) LCM results; (b) HCM results.

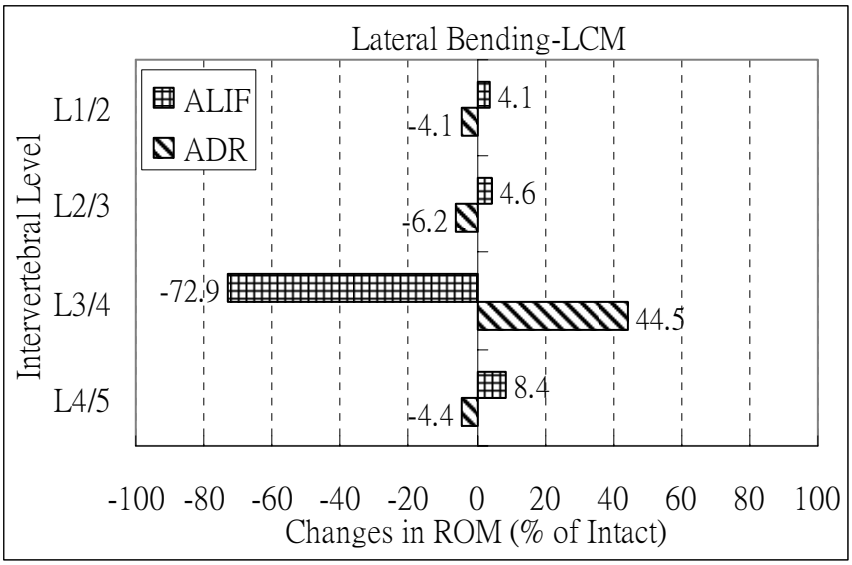

(a)

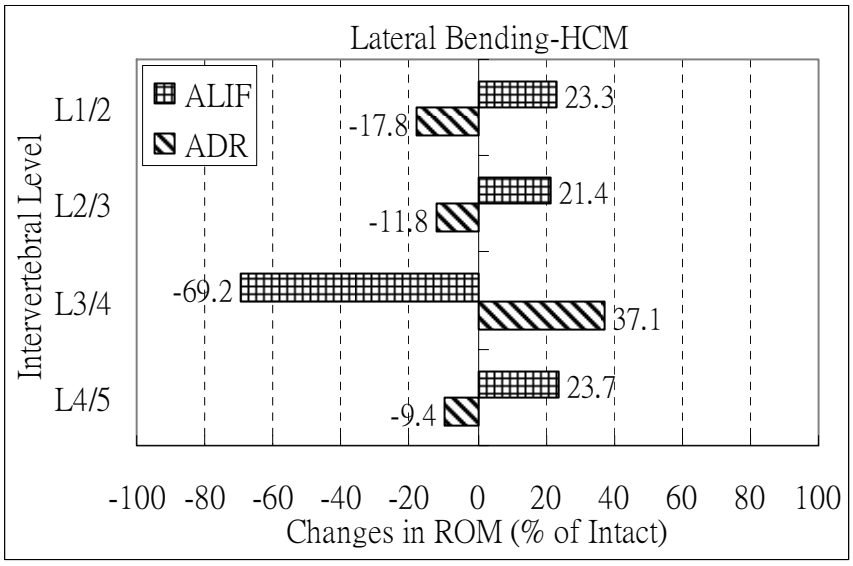

(b)

Figure 4.5: Changes in the ROM under lateral bending: (a) LCM results; (b) HCM results.

4.3. Facet Contact Force under Extension and Torsion

Implant Level Effects

Under the LCM, the ALIF model showed no FCF in extension; the FCF was obviously reduced in torsion (-73.8 %), compared with the INT model. In contrast, the ADR model had a large increase in FCF in extension (+44.2 %) (Figure 4.6(a)) and torsion (+38.7 %) (Figure 4.7(a)). The FCF values of the LCM are listed in Table 4.1.

Under the HCM, the ALIF model also showed no FCF in extension; the FCF was obviously reduced in torsion (-54.0 %) compared to the INT model. The ADR model had a small FCF increase in extension (+4.9 %) (Figure 4.6(b)) and in torsion (+5.1 %) (Figure 4.7(b)). The FCF values of the HCM are listed in Table 4.1.

Both control methods can provide similar results in the ALIF model. However, the LCM indicated a greater decrease in the FCFs in torsion than the HCM (-73.8 % vs. -54.0 %). In the ADR model, the LCM prominently showed FCFs increase in both extension and torsion compared to the HCM. Contrary to the LCM, the HCM revealed FCFs close to those of the INT model in both extension and torsion.

It is known that posterior interbody fusion often combines with posterior decompression to relieve low back pain. Therefore, there is no FCF at the implant level in most posterior interbody fusion cases due to resectioning of the facet joint and surrounding bony tissue following the decompression surgery. In the present ALIF model, the FCF was found under torsion due to the preservation of the facet joint; however, the value of the FCF is still much lower than in the INT model, regardless of whether the LCM or HCM is used. Based on these results, the present study indicates that facet pathology at the implant level might not occur after treatment by 360^{o} spinal fusion. Several biomechanical studies have demonstrated that a cross-link configuration provides increased torsional stiffness as compared with unlinked configurations

[98-99]. If surgeons are still worried about these small FCFs, the cross-linked pedicle screw fixation is an option for the elimination of torsional FCFs.

Unlike fusion techniques, total disc replacement has shown inconsistent results in clinical reports concerning facet problems at the implant level. Several studies have demonstrated no changes or only a few facet joint pathology changes at the implant level following the use of an artificial disc [46, 50, 100]. However, some reports indicated complications following implantation of an artificial disc, including degeneration of the facet joint at the implant level, with use of either a ball-and-socket or a mobile core design. Rates of degeneration ranged from 11% to 36.4% [47, 101, 102]. Punt *et al.* [103] indicated that high percentages (33% of 75 patients) of patients need one or more reoperations due to facet joint degeneration after implantation of an artificial disc. These conflicting results may be due to many factors, such as the size of the implant, patient selection, multi-level replacement, evaluation method, mal-alignment of implant, length of follow-up period, imprecise diagnostic criteria, various biological changes, and technical errors during surgery. In addition, several biomechanical studies reported that facet joint problems may occur after the removal of the anterior longitudinal ligament and the annulus fibrosis, for both designs of artificial disc [78, 104-107].

In the present ADR model, the anterior longitudinal ligament was concerned to be resutured; however, a prominently higher FCF at the implant level was still revealed under the LCM. Contrary to the LCM, the FCF was close to the INT model under the HCM. Goel *et al.*'s [71] FE study also demonstrated that the FCFs across the implanted level showed a 14% increase in extension for the LCM as opposed to a 13.4% decrease for the HCM, in comparison to data from the intact model. They believed that the LCM is not as clinically relevant as the HCM. Thus, their conclusion implied that the use of an artificial disc would not affect facet joint load at the implant level. Based on the hypotheses of clinical relevance for both the LCM and HCM mentioned above, the present study

indicates an increased likelihood of accelerative degeneration of the facet joint at the implant level under the LCM prediction. It implies a higher risk for facet joint degeneration at the implant level due to the patient's normal lift work-loading condition after implantation of an artificial disc. Therefore, the present study suggests that artificial discs are not suitable for laborer population or overweight patients. In other words, patients who have undergone implantation of an artificial disc should avoid high external loading under extension and torsion when normal activities are resumed post-surgery. To avoid high FCF at the implant level, the present study recommends a new artificial disc design to constrain limited motion in extension and torsion.

Adjacent Level Effects

The ALE% of the FCF was defined as the averaged percentage change of the FCF from whole, non-operated levels. Under the LCM, the ALE% of the ALIF model in extension (+45.8 %) increased prominently. However, there were only minor increases in torsion (+4.4 %). The ALE% values of the ADR model were close to those of the INT model in extension (+7.6 %) (Figures 4.6(a)) and torsion (+2.4 %) (Figures 4.7(a)).

Under the HCM, the ALE% of the ALIF model increased in extension (+148.2 %) and torsion (+37.5 %), as compared with the INT model. In contrast, the ALE% of the ADR model decreased in extension (-32.6 %) (Figures 4.6(b)) and torsion (-20.2 %) (Figures 4.7(b)), as compared with the INT model.

For the FCF, the HCM increased the ALE% more than when using the LCM in the ALIF model. On the other hand, the HCM decreased the ALE% more than when using the LCM in the ADR model.

Accelerative degeneration of adjacent levels is an important clinical issue after spinal fusion. Etebar *et al.* [34] reported 14.4% of patients developed ASD after undergoing fusion. Some 33% of these ASD patients had spinal canal stenosis due to disc herniation and/or facet hypertrophy. Lee [31] demonstrated

that the most common pathological condition at the adjacent level was hypertrophic degenerative arthritis of the facet joints (16 of 18 patients). Comparing both loading conditions in the present study, the HCM increased the ALE% on facet joints more than when using the LCM in the ALIF model. The result of FCFs under the HCM prediction is in good agreement with clinical findings, which might be related to adjacent facet joint degeneration following spinal fusion. Therefore, the present study suggests that the HCM is more clinically relevant to predict the accelerative degeneration of facet joints at adjacent levels. Based on the hypotheses of clinical relevance for both the LCM and HCM mentioned above, the present study implies a higher risk for facet joint degeneration at adjacent levels due to the patient's daily life motions during restoration after spinal fusion. Therefore, the present study suggests that patients who have undergone treatment by spinal fusion should avoid excessive or frequent motion, especially extension and torsion, as normal activities are resumed post-surgery.

To the best of our knowledge, facet joint degeneration at the adjacent level after implantation of an artificial disc was only reported by van Ooij [102]. Their study indicated that the main cause of persistent complaint was facet joint arthrosis in 11 patients (11 of 27 patients). In a few of these cases, adjacent levels were also affected by facet joint degeneration. In the present ADR model, the LCM slightly increased the ALE% of the facet joint and the HCM prominently decreased the ALE% of the facet joint. These results did not indicate remarkably higher FCFs than the INT model at the adjacent levels after using an artificial disc, regardless of whether the LCM or HCM was used. Therefore, the present study indicates that a lower risk of accelerative degeneration at the adjacent facet joints after insertion of an artificial disc due to unobvious or decreased ALEs.

Table 4.3: Facet contact forces among the INT, ALIF, and ADR models at the implant and adjacent levels under both the LCM and HCM are listed.

Unit: N

Loading Conditions	Motions	Models	Facet Contact Forces (N)			
			L1-L2	L2-L3	L3-L4	L4-L5
LCM						
	Extension*	INT	33.67	47.24	72.90	69.06
		ALIF	50.63	68.03	0	98.81
		ADR	42.87	47.13	105.15	66.13
	Left Torsion*	INT	121	129.58	125.09	126.73
		ALIF	122.85	136.2	32.78	135.26
		ADR	125.51	129.13	173.55	131.61
HCM						
	Extension*	INT	33.67	47.24	72.90	69.06
		ALIF	90.59	117.24	0	156.93
		ADR	23.41	30.28	76.48	47.34
	Left Torsion*	INT	121	129.58	125.09	126.73
		ALIF	160.65	178.38	57.51	180.01
		ADR	98.24	101.12	131.51	101.52

*The facet contact forces in extension and left torsion were collected from the right facet joint.

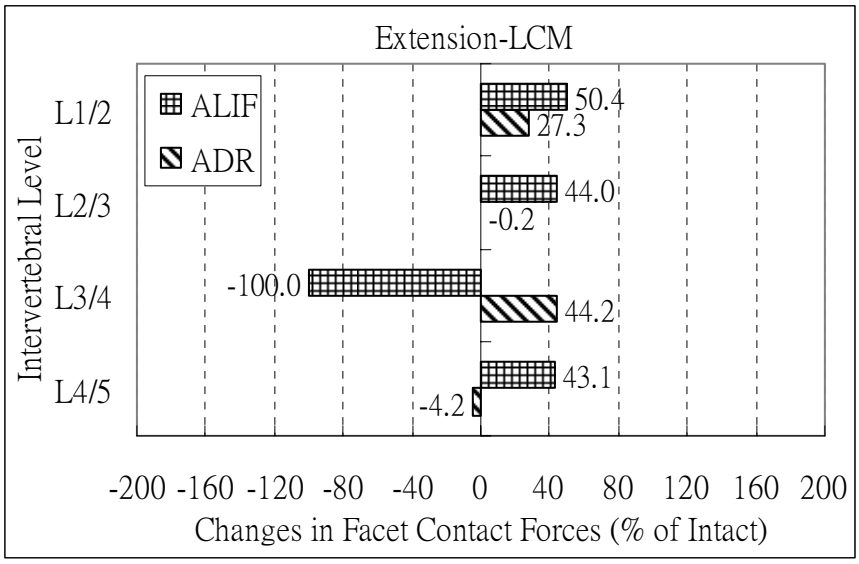

(a)

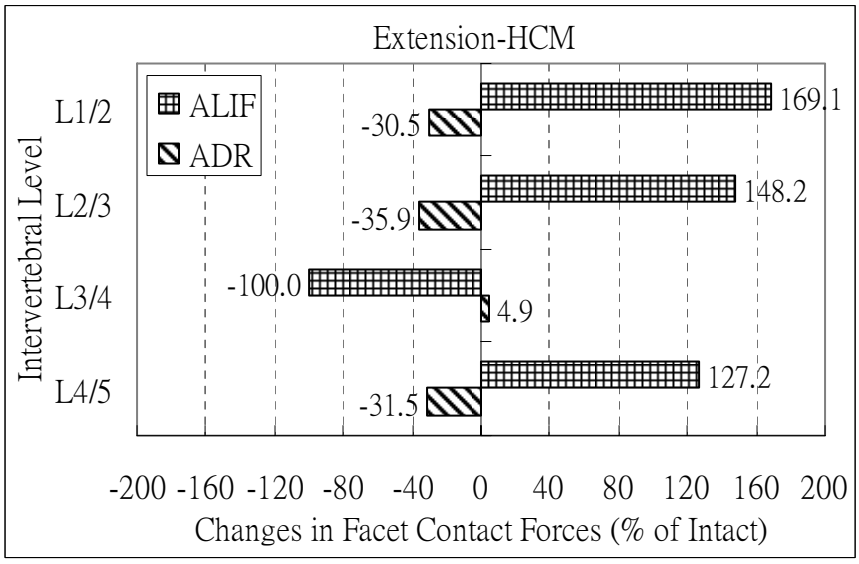

(b)

Figure 4.6: Changes in the facet contact forces under extension: (a) LCM results; (b) HCM results.

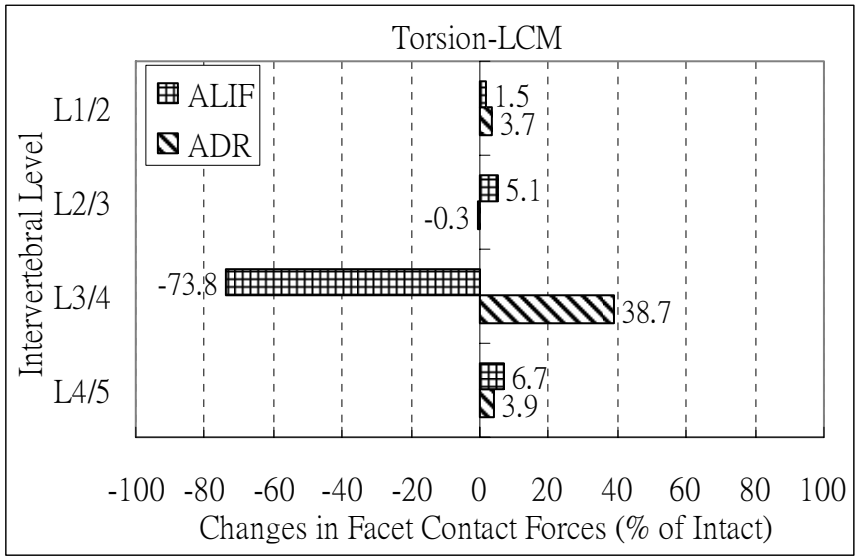

(a)

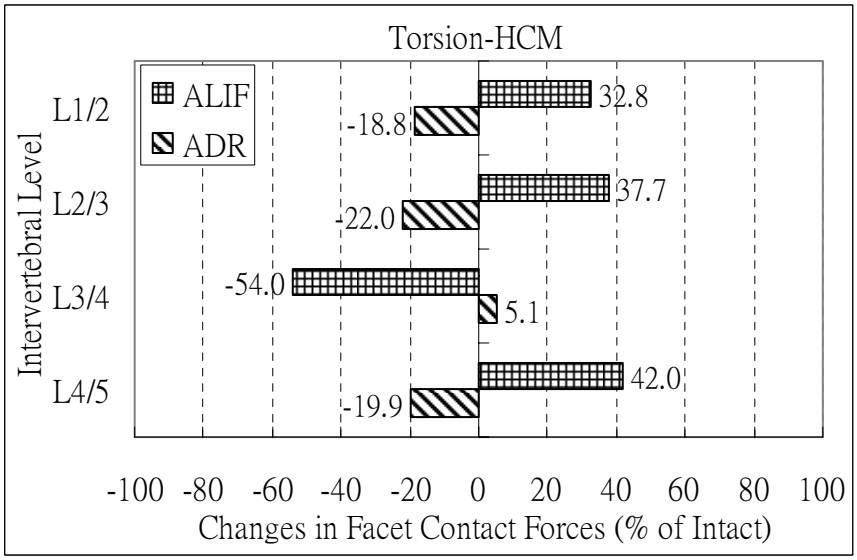

(b)

Figure 4.7: Changes in the facet contact forces under torsion: (a) LCM results; (b) HCM results.

4.4. von Mises Stress Distribution in the Adjacent Disc Annulus

The von Mises stress distribution of the L2/3 adjacent disc annulus in the three FE models for the LCM and the HCM are shown in Figure 4.8 (flexion), Figure 4.9 (extension), Figure 4.10 (torsion), and Figure 4.11 (lateral bending).

Under the LCM, the stress distribution pattern of the adjacent disc annulus in the ALIF model was close to that of the INT model; small stress increases were found in flexion and torsion, and small stress decreases were found in extension and lateral bending, compared with the INT model. For the ADR model, the stress distribution pattern changed and was dissimilar to the INT model in extension and torsion: The dotted arrows (Figure 4.9 and Figure 4.10) indicate that annulus stress during extension (Figure 4.9) was increased at the posterior-outer layer of the annulus regions close to the inferior side of the endplate, the anterior-inner layer of the annulus regions, and redistributed at posterior-lateral annulus regions; during left torsion (Figure 4.10), annulus stress was redistributed and increased at the right anterolateral- and posterolateral-inner sites of the annulus regions, compared with the INT model.

Under the HCM, the stress increased more obviously at the L2/3 adjacent annulus in the ALIF model. The solid arrows (Figure 4.8 to Figure 4.11) indicate that annulus stress during flexion (Figure 4.8) was concentrated at the anterior- and posterior-outer layers of the annulus regions close to both sides of the endplate, and the anterior-inner layer of the annulus regions. During extension (Figure 4.9), annulus stress was concentrated at the posterior-outer layer of the annulus regions close to the inferior side of the endplate, the anterior-outer layer of the annulus regions close to the superior side of the endplate, and the anterior-inner layer of the annulus regions. During torsion (Figure 4.10), annulus stress was concentrated at the circumferential ring of the annulus regions close to the endplate. During lateral bending (Figure 4.11), annulus stress was concentrated at the left and right lateral-outer layers of the annulus regions close to the endplate. For the ADR model, stress concentration at the L2/3 adjacent

level was not obvious, and the stress pattern was close to that of the INT model; however, the stress decreased more obviously at the L2/3 annulus in extension and torsion.

Overall, for the LCM, the stress distribution pattern at the adjacent L2/3 annulus changed and increased in other annulus regions under extension and torsion following implantation of a total disc replacement, compared with the INT model; these two motions also resulted in a higher stress increase when compared with the HCM. For the HCM, a higher stress concentration at the adjacent L2/3 annulus was more clearly shown under four physiological motions following a fusion procedure, compared with the LCM.

Clinical reports have demonstrated that high incidences of accelerative disc degeneration at the adjacent level following spinal fusion ranged from 5.2% to 61%; these reports are described in detailed in Chapter 2 [3, 16, 33-35]. In the present study, the solid arrows indicate that the stress on the adjacent disc annulus increased markedly and was concentrated at a number of regions under the HCM for the ALIF model (Figure 4.8 to 4.11); this result under the HCM seems to trend toward the clinical finding of adjacent disc degeneration, in contrast to the findings of the LCM. Based on these observations, these high stress regions might be correlated with accelerative disc degeneration at adjacent levels. Therefore, the present study suggests that the HCM is more effective and clinically relevant in predicting the ALEs of a disc due to an increase of stress after spinal fusion.

The surgical goals of total disc replacement are to restore normal physiological motion and to avoid disc degeneration at adjacent levels. However, it is still not clear whether total disc replacement causes adjacent disc degeneration or not. Some clinical reports have demonstrated that total disc replacement has an associated high incidence of adjacent disc degeneration [47, 49], while some reports did not [46, 48, 50]. Currently, only one prospective study reported ASD complications with total disc replacements versus lumbar

fusions [50]. This report indicated that disc replacement patients (8 %) reached a statistically lower rate of long-term ASD disease as compared with fusion patients (20.9 %). Mulholland and Sengupta [108] indicated that abnormal patterns of loading rather than abnormal movement are the reason that disc degeneration causes back pain in some patients. Based on this theory, ROM is not suitable for predicting ASD disease, and the stress distribution pattern should be more clinically relevant. Adjacent annulus stress of the ADR model indicates that annulus stresses are markedly lower than in the INT model under the HCM prediction. However, the dotted arrows indicate that the stress distribution patterns changed and increased in other annulus regions under the LCM prediction, especially for extension and torsion, compared with the INT model (Figure 4.9 to 4.10). Based on these observations, these changed stress patterns might relate to accelerative disc degeneration at adjacent levels. Therefore, the present study concluded that adjacent disc degeneration might be induced by abnormal stress patterns after total disc replacement; however, the risk of adjacent disc degeneration is lower than in spinal fusion.

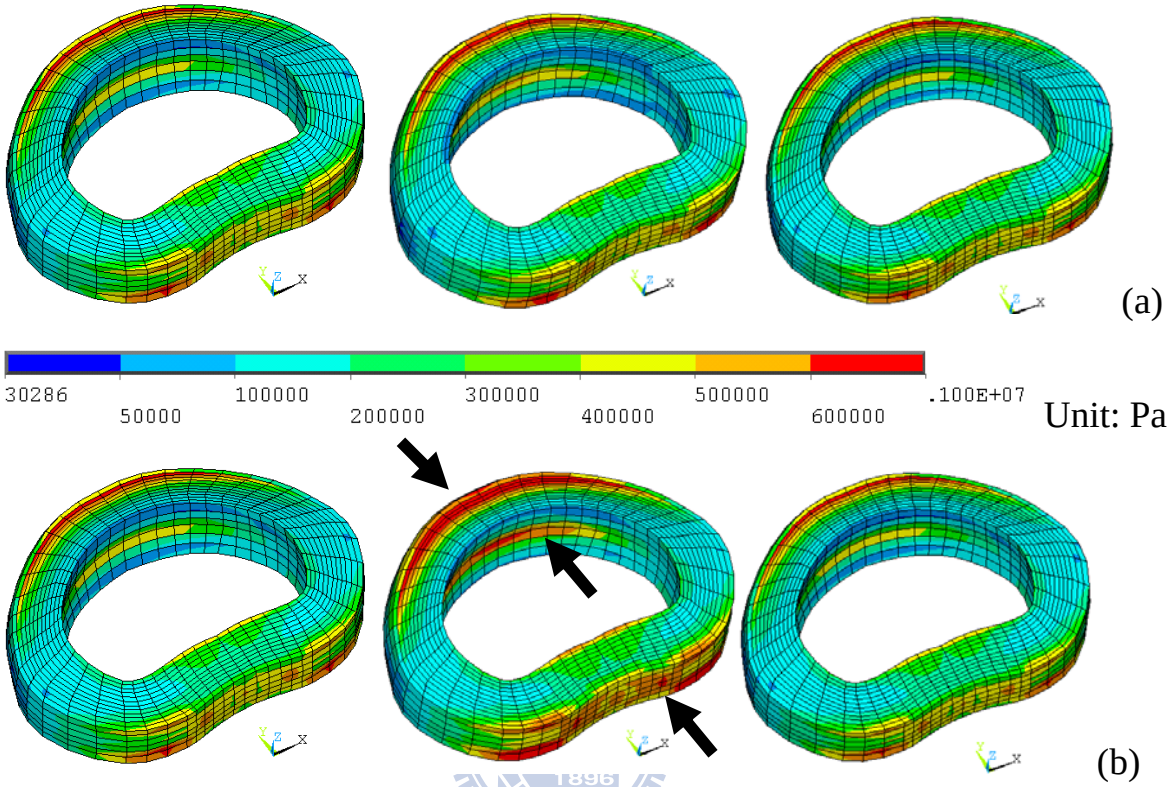

Figure 4.8: The von Mises stress distribution of the adjacent L2/L3 disc annulus under flexion for the INT model (left), the ALIF model (middle) and the ADR model (right): (a) LCM; (b) HCM. The solid arrows indicate stress concentration regions.

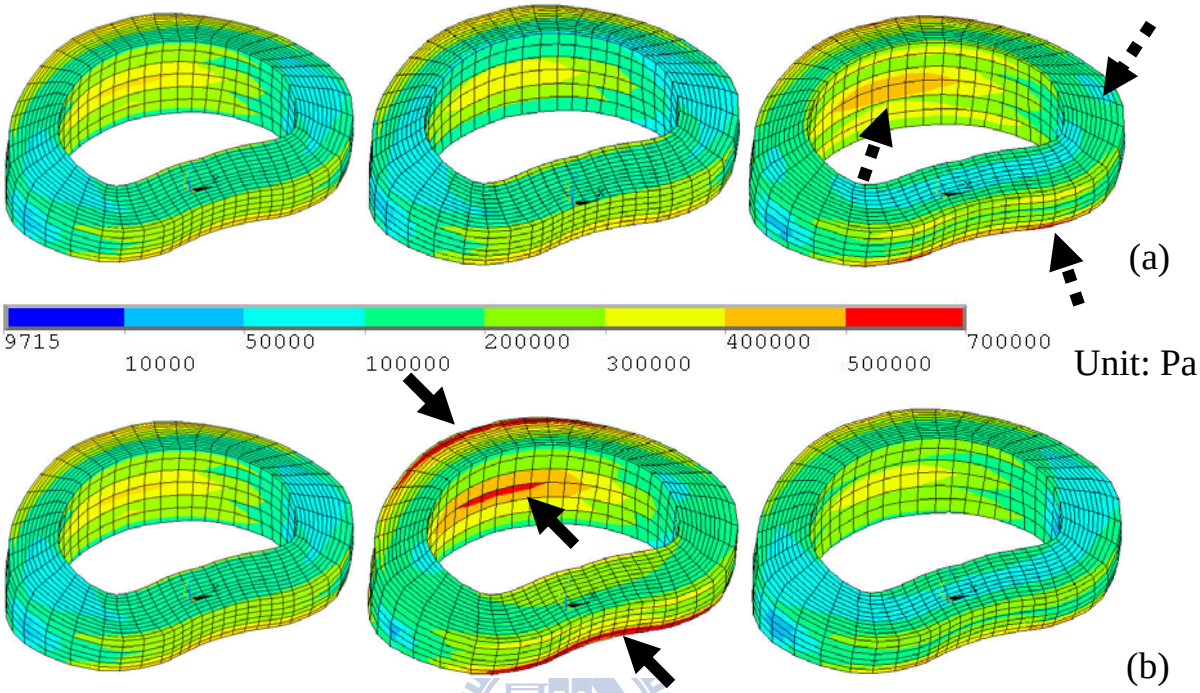

Figure 4.9: The von Mises stress distribution of the adjacent L2/L3 disc annulus under extension for the INT model (left), the ALIF model (middle), and the ADR model (right): (a) LCM; (b) HCM. The solid arrows indicate stress concentration regions. The dotted arrows indicate the regions where the stress distribution pattern changed.

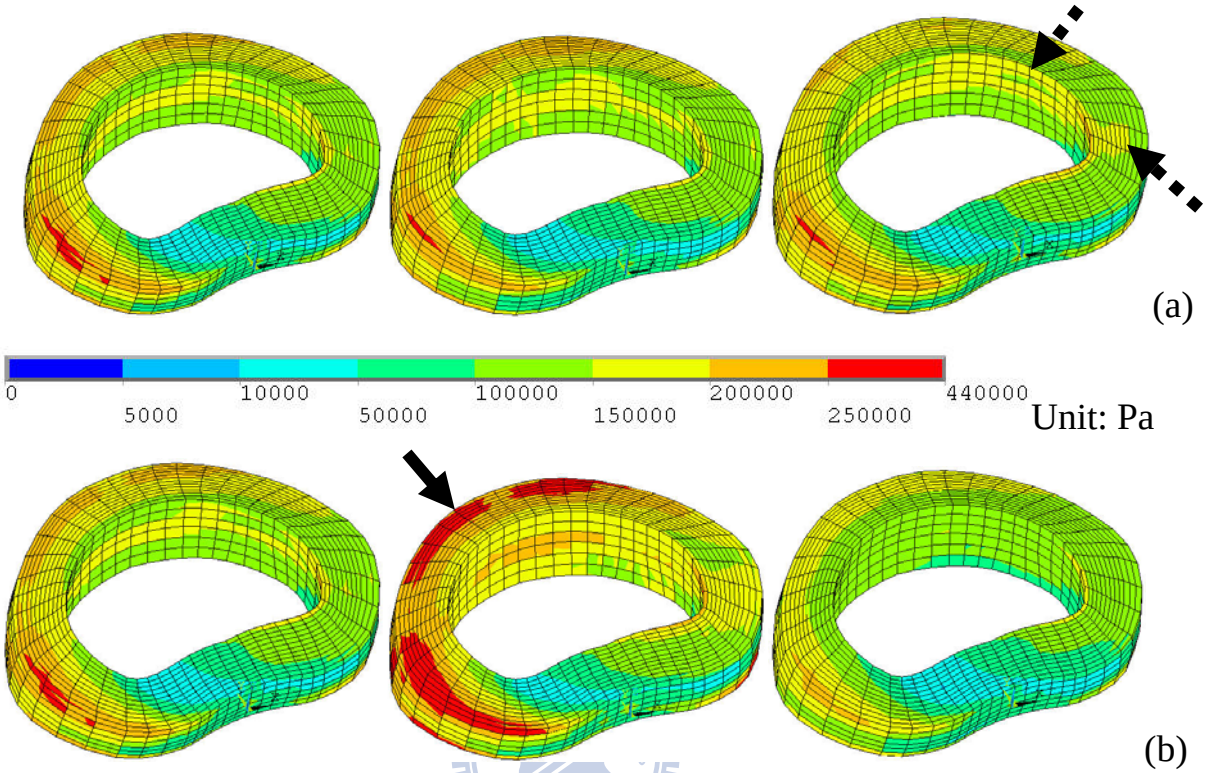

Figure 4.10: The von Mises stress distribution of the adjacent L2/L3 disc annulus under torsion for the INT model (left), the ALIF model (middle), and the ADR model (right): (a) LCM; (b) HCM. The solid arrows indicate stress concentration regions. The dotted arrows indicate the regions where the stress distribution pattern changed.

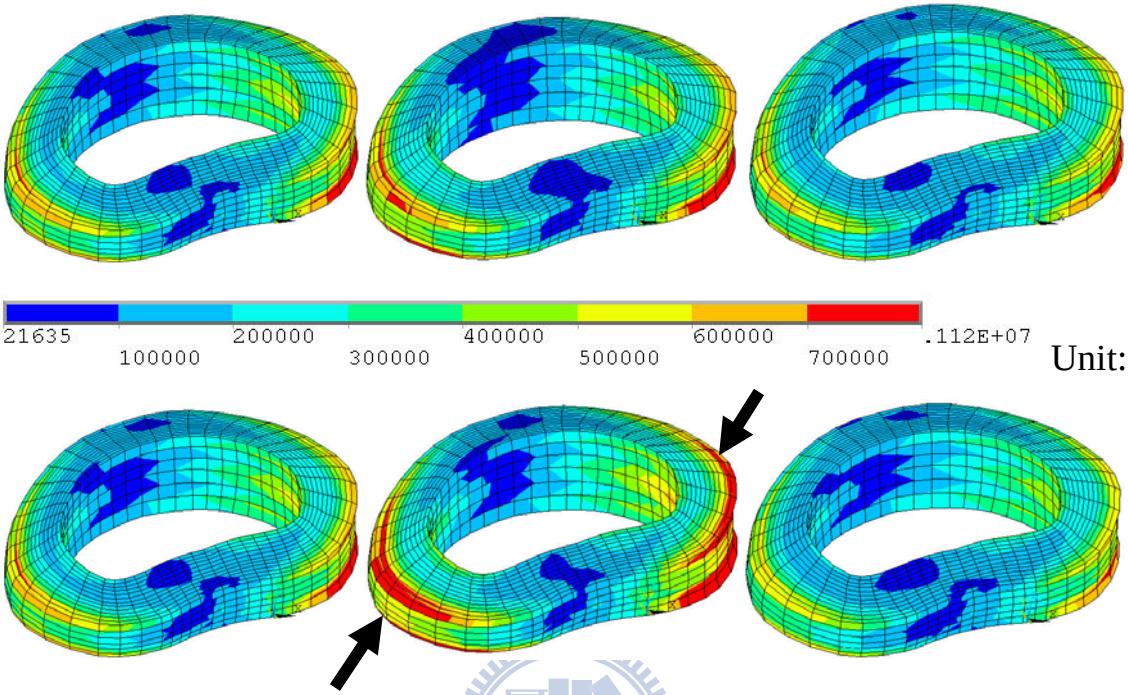

Figure 4.11: The von Mises stress distribution of the adjacent L2/L3 disc annulus under lateral bending for the INT model (left), the ALIF model (middle), and the ADR model (right): (a) LCM; (b) HCM. The solid arrows indicate stress concentration regions.

4.5. Limitations of the Present Study

One limitation of this study is that the material properties of this simulation, such as the nonlinear behavior of spinal ligaments, the viscoelasticity of the disc, and the grade of the degenerative disc, were slightly simplified and idealized from those of a cadaver specimen. A degenerative disc is common in many patients before surgery. The various grades of degeneration in the disc, such as delamination, dehydration or reduced disc height, do not allow for exact replication of the unique material properties of a degenerated disc. Therefore, normal material properties were used in this simulation.

In a real spine, the size of vertebrae and the orientation of the facet joint are different depending on each segment [109, 110]. The influence of geometry was not considered here, which might affect the absolute values of the vertebral stresses and facet joint loads. Also, the constrained behavior used in the bone-screw interface, the thread of the pedicle screw, the keel in the metallic plates of the ProDisc, and the bone ingrowth into the cage were simplified. Pretension should occur after inserting the ADR, which might distract the remaining annulus, reducing the ROM and facet loading at the implant level. This mechanism was not modeled here, which is a further limitation of this study.

The loading conditions of these FE simulations were similar to those of the traditional *in vitro* test, so the muscle contraction, complicated external load, and movement of the pelvis were not considered in this study. During normal daily activities, muscles induce considerably high compression forces on the lumbar spine [111] and play a very important role in stabilizing the lumbar spine [112]. The absence of muscle forces would lead to more instability, especially at the implant level of surgery models. In addition, the annulus stress and implant loading would be much lower than those measured *in vivo*.

Chapter 5: Conclusion and Future Work

Final suggestions are provided for understanding which testing protocol is suitable for understanding the physical effects of spinal implants. In addition, several topics that can be extended from this research are introduced in this chapter.

5.1. Conclusion

This research has made two notable contributions to the field. First, a five-level lumbar spine FE model was constructed and validated. This lumbar spine FE model can be used in future studies for evaluation of various spinal implants, spinal surgical techniques, and spinal diseases. Second, differences between the LCM and HCM for the evaluation of an anterior interbody fusion cage and an artificial disc were observed and explained.

At the implant level, this study suggests that both control methods can be adopted to predict the fusion model, and similar stabilization characteristics can be found. The LCM emphasized the effects of the non-fusion device at the implant level. At adjacent levels, the HCM emphasized the effects of the fusion device. By comparing present data with clinical findings, it can be observed that the LCM is more effective and clinically relevant in evaluating accelerative degeneration of facet joints at the implant level after insertion of an artificial disc. The HCM is more effective and clinically relevant in evaluating accelerative degeneration of the discs and facet joints at adjacent levels after insertion of a spinal cage. In addition, this study demonstrated that the use of stress distribution patterns to predict adjacent disc degeneration is better than using the ROM, especially in cases of total disc replacement.

This study suggests that these two analytical methods can be used to predict specific conditions in a patient's daily life. The HCM is suitable for evaluation of the patient's daily life motions during restoration after surgery. The LCM is

suitable for evaluation of the patient's normal lift work-loading condition after surgery.

5.2. Future Work

This study suggests several avenues for future research. The five-level lumbar spine model derived in this study can be used in parameter analysis for creating a design guide which could include the effects of implant height, position, material, size, and shape. The results are useful for engineers in the design and development of new spinal implants. It also serves as a reference resource for surgeons in selecting implants for the patients. To avoid accelerative disc degeneration after treatment by spinal fusion, several pedicle-based non-fusion dynamic stabilization systems have been developed. Differences between dynamic stabilization systems and traditional pedicle screw instrumentation systems can be considered in future studies. In addition, patients who had accelerative disc degeneration at adjacent levels could be treated with various non-fusion spinal implants to prevent another surgery for extended fusion to the adjacent levels. The function of hybrid use of these spinal implants can be investigated through further study. In addition, the advantage of non-fusion spinal implants is to preserve a mildly to moderately degenerative disc. Therefore, the various grades of degeneration in the disc could be considered through change of material properties, disc height, or disc geometry.

Recently, Patwardhan *et al.* [113] proposed a "follower load" to mimic the more realistic physiological compressive loads seen *in vivo*. This consists of a compressive load applied along a "follower load" path that approximates the tangent to the curve of the lumbar spine, thus subjecting the whole lumbar spine to nearly pure compression. Besides the "follower load", there are several methods that have been presented for mimicking the role of muscles. Differences among them are still not known. Therefore, comparison of these loading conditions is another topic for future work.

References

[1] Anderson GB. Epidemiological features of chronic low-back pain. Lancet. 1999;14;354:581-5.

[2] Weinstein JN, Lurie JD, Olson PR, et al. United States' trends and regional variations in lumbar spine surgery: 1992-2003. Spine. 2006;31:2707-14.

[3] Park P, Garton HJ, Gala VC, et al. Adjacent segment disease after lumbar or lumbosacral fusion: review of the literature. Spine. 2004;29:1938-44.

[4] German JW, Foley KT. Disc arthroplasty in the management of the painful lumbar motion segment. Spine. 2005;30:S60-7.

[5] McBroom RJ, Hayes WC, Edwards WT, et al. Prediction of vertebral body compressive fracture using quantitative computed tomography. J Bone Joint Surg Am. 1985;67:1206-14.

[6] Gower WE, Pedrini V. Age-related variations in proteinpolysaccharides from human nucleus pulposus, annulus fibrosus, and costal cartilage. J Bone Joint Surg Am. 1969;51:1154-62.

[7] Panagiotacopulos ND, Pope MH, Krag MH, et al. Water content in human intervertebral discs. Part I. Measurements by magnetic resonance imaging. Spine. 1987;12:912-7.

[8] Marchand F, Ahmed AM. Investigation of the laminate structure of lumbar disc annulus fibrosus. Spine. 1990;15:402-10.

[9] Adams M, Bogduk N, Burton K, et al. The biomechanics of back pain, 2nd edition, Churchill Livingstone, Edinburgh, 2006.

[10] Skaggs DL, Weidenbaum M, Iatridis JC, et al. Regional variation in tensile properties and biochemical composition of the human lumbar annulus fibrosus. Spine. 1994;19:1310-9.

[11] Setton LA, Zhu W, Weidenbaum M, et al. Compressive properties of the cartilaginous end-plate of the baboon lumbar spine. J Orthop Res.

1993;11:228-39.

[12] Ahmed AM, Duncan NA, Burke DL. The effect of facet geometry on the axial torque-rotation response of lumbar motion segments. Spine. 1990;15:391-401.

[13] Panjabi MM, Goel VK, Takata K. Physiologic strains in the lumbar spinal ligaments. An in vitro biomechanical study 1981 Volvo Award in biomechanics. Spine. 1982;7:192-203.

[14] Hall SJ. Basic Biomechanics, 4th edition, McGraw-Hill, New York, 2004.

[15] Zucherman J, Hsu K, Picetti G, et al. Clinical efficacy of spinal instrumentation in lumbar degenerative disc disease. Spine. 1992;17:834-7.

[16] Brantigan JW, Neidre A, Toohey JS. The lumbar I/F cage for posterior lumbar interbody fusion with the variable pedicle screw placement system: 10-year results of a Food and Drug Administration clinical trial. Spine J. 2004;4:681-8.

[17] Eule JM, Breeze R, Kindt GW. Bilateral partial laminectomy: A treatment for lumbar spinal stenosis and midline disc herniation. Surg Neurol. 1999;52:329-38.

[18] Hibbs RH. An operation for progressive spinal deformities. New York Med J. 1911;93:1013-6.

[19] Herkowitz HN, Garfin SR, Balderston RA, et al. Rothman-Simeone the spine, 4th edition, Harcourt Publishers International Company, Singapore, 1999.

[20] McAfee PC. Interbody fusion cages in reconstructive operations on the spine. J Bone Joint Surg Am. 1999;81:859-80.

[21] Stauffer RN, Coventry MB. Anterior interbody lumbar spine fusion. Analysis of Mayo Clinic series. J. Bone Joint Surg. Am 1972;54:756-768.

[22] Dennis S, Watkins R, Landaker S, et al. Comparison of disc space heights after anterior lumbar interbody fusion. Spine. 1989;14:876-878.

[23]http://www.spine-health.com/treatment/spinal-fusion/anterior-lumbar-interbody-fusion-alif-surgery

[24]http://www.spine-health.com/treatment/back-surgery/posterior-lumbar-interbody-fusion-plif-surgery

[25] Ames CP, Acosta FL, Chi J, et al. Biomechanical compsrison of posterior lumbar interbody and transforaminal lumbar interbody fusion performed at 1 and 2 levels. Spine. 2005;30:E562-6.

[26] Ray CD. Threaded titanium cages for lumbar interbody fusions. Spine. 1997;22:667-80.

[27] Brantigan JW, Steffee AD, Lewis ML, et al. Lumbar interbody fusion using the Brantigan I/F cage for posterior lumbar interbody fusion and the variable pedicle screw placement system: Two-year results from a Food and Drug Administration Investigational Device Exemption clinical trial. Spine. 2000;25:1437-46.

[28] Kuslich SD, Danielson G, Dowdle JD, et al. Four-year follow-up results of lumbar spine arthrodesis using the Bagby and Kuslich lumbar fusion cage. Spine. 2000;25:2656-62.

[29] Yuan HA, Kuslich SD, Dowdle JA, et al. Prospective multicenter clinical trial of the BAK interbody fusion system. Annual Meeting of the North American Spine Society, New York, 1997.

[30] Anjarwalla N, Morcom RK, Fraser RD. Supplementary stabilization with anterior lumbar intervertebral fusion: A radiologic review. Spine. 2006;31:1281-7.

[31] Lee CK. Accelerated degeneration of the segment adjacent to a lumbar fusion. Spine. 1988;13:375-7.

[32] Lehmann TR, Spratt KF, Tozzi JE, et al. Long-term follow-up of lower lumbar fusion patients. Spine. 1987;12:97-104.

[33] Rahm MD, Hall BB. Adjacent segment degeneration after lumbar fusion with instrumentation: A retrospective study. J Spinal Disord. 1996;9:392-400.

[34] Etebar S, Cahill DW. Risk fractures for adjacent segment failure following lumbar fixation with rigid instrumentation for degenerative instability. J

Neurosurg. 1999;90:163-9.
[35] Aota Y, Kumano K, Hirabayashi S. Post-fusion instability at the adjacent segments after rigid pedicle screw fixation for degenerative lumbar spinal disorders. J Spinal Disord. 1995;8:464-73.
[36] Kumar MN, Baklanov A, Chopin D. Correlation between sagittal plane changes and adjacent segment degeneration following lumbar spine fusion. Eur Spine J. 2001;10:314-9.
[37] Mayer HM, Korge A. Non-fusion technology in degenerative lumbar spinal disorders: facts, questions, challenges. Eur Spine J. 2002;11:S85-91.
[38] Weber BG. Zwischenwirbel Totaprothese, Swiss Patent 624573, 1978.
[39] Bao QB, McCullen GM, Higham PA, et al. The artificial disc: theory, design and materials. Biomaterials. 1996;17:1157-67.
[40] Lee CK, Goel VK. Artificial disc prosthesis: design concepts and criteria. Spine J. 2004;4:S209-18.
[41] Galbusera F, Bellini CM, Zweig T, et al. Design concepts in lumbar total disc arthroplasty. Eur Spine J. 2008;17:1635-50.
[42] Huang RC, Girardi FP, Cammisa GF, et al. The implications of constraint in lumbar total disc replacement. J Spinal Disord Tech. 2003;16:412-7.
[43] Delamarter RB, Fribourg DM, Kanim LE, et al. ProDisc artificial total lumbar disc replacement: Introduction and early result from the United States clinical trial. Spine. 2003;28:S167-75.
[44] Zigler JE. Clinical results with ProDisc: European experience and U.S. investigation device exemption study. Spine. 2003;28:S163-6.
[45] Bertagnoli R, Kumar S. Indications for full prosthetic disc arthroplasty: a correlation of clinical outcome against a variety of indications. Eur Spine J. 2002;11:S131-6.
[46] Siept CJ, Mayer M, Wiechert K, et al. Clinical results of total lumbar disc replacement with ProDisc II. Spine. 2006;31:1923-32.
[47] Shim CS, Lee SH, Shin HD, et al. CHARITE Versus ProDisc: A

Comparative Study of a Minimum 3-Year Follow-up. Spine. 2007;32:1012-8.
[48] Marnay T. Lumbar disc replacement: 7-11 years results with Pro-disc. Eur Spine J. 2002;11:S19.
[49] Huang RC, Tropiano P, Marney T, et al. Range of motion and adjacent level degeneration after lumbar total disc replacement. Spine J. 2006;6:242-7.
[50] Guyer RD, McAfee PC, Banco RJ, et al. Prospective, randomized, multicenter food and drug administration investigational device exemption study of lumbar total disc replacement with the CHARITE artificial disc versus lumbar fusion: Five-year follow-up. Spine J. 2009;9:374-86.
[51] Fraser RD, Ross ER, Lowery G, et al. AcroFlex design and results. Spine J. 2004;4:S245-51.
[52] Singh K, Vaccaro AR, Albert TJ. Assessing the potential impact of total disc arthroplasty on surgeon practice patterns in North America. Spine J. 2004;4:S195-201.
[53] Cunningham BW, Gordon JD, Dmitriev AE, et al. Biomechanical evaluation of total disc replacement arthroplasty: An in vitro human cadaveric model. Spine. 2003;28:S110-7.
[54] Sudo H, Oda I, Abumi K, et al. Biomechanical study on the effect of five different lumbar reconstruction techniques on adjacent-level intradiscal pressure and lamina strain. J Neurosurg Spine. 2006;5:150-5.
[55] Rao RD, David KS, Wang M. Biomechanical changes at adjacent segments following anterior lumbar interbody fusion using tapered cages. Spine. 2005;30:2772-6.
[56] Chow DH, Luk KD, Evans JH, et al. Effects of short anterior lumbar interbody fusion on biomechanics of neighboring unfused segments. Spine. 1996;21:549-55.
[57] Shono Y, Kaneda K, Abumi K, et al. Stability of posterior spinal instrumentation and its effects on adjacent motion segments in the lumbosacral spine. Spine. 1998;23:1550-8.

[58] Cunningham BW, Kotani Y, McNulty PS, et al. The effect of spinal destabilization and instrumentation on lumbar intradiscal pressure: an in vitro biomechanical analysis. Spine. 1997;22:2655-63.

[59] Weinhoffer SL, Guyer RD, Herbert M, et al. Intrediscal pressure measurements above an instrumented fusion. A cadaveric study. Spine. 1995;20:526-31.

[60] Denoziere G, Ku DN. Biomechanical comparison between fusion of two vertebrae and implantation of an artificial intervertebral disc. J Biomech. 2006;39:766-75.

[61] Schmoelz W, Huber JF, Nydegger T, et al. Influence of a dynamic stabilization system on load bearing of a bridged disc: An in vitro study of intradiscal pressure. Eur Spine J. 2006;15:1276-85.

[62] Rohlmann A, Neller S, Bergmann G, et al. Effect of an internal fixator and a bone graft on intersegmental spinal motion and intradiscal pressure in the adjacent reions. Eur Spine J. 2001;10:301-8.

[63] Rohlmann A, Calisse J, Bergmann G, et al. Internal spinal fixator stiffness has only a minor influence on stresses in the adjacent discs. Spine. 1999;24:1192-6.

[64] Schmoelz W, Huber JF, Nydegger T, et al. Dynamic stabilization of the lumbar spine and its effects on adjacent segments: an in vitro experiment. J Spinal Disord Tech. 2003;16:418-23.

[65] Panjabi MM, Brand RA, White AA. Three-dimensional flexibility and stiffness properties of the human thoracic spine. J Biomech. 1976;9:185-92.

[66] Panjabi MM. Hybrid multidirectional test method to evaluate spinal adjacent-level effects. Clin Biomech. 2007;22:257-65.

[67] Goel VK, Panjabi MM, Patwardhan AG, et al. Test protocols for evaluation of spinal implants. J Bone Joint Surg Am. 2006;88:103-9.

[68] Grassmann S, Oxland TR, Gerich U, et al. Constrained testing conditions affect the axial rotation response of lumbar functional spinal units. Spine.

1998;23:1155-62.
[69] Panjabi MM, Kato Y, Hoffman H, et al. A study of stiffness protocol as exemplified by testing of a burst fracture model in sagittal plane. Spine. 2000;25:2748-54.
[70] Panjabi MM. Biomechanical testing to identify adjacent-level effects. Iv World Congress of Biomechanics, Calgary, Canada, August 4-9, 2002.
[71] Goel VK, Grauer JN, Patel Tch, et al. Effects of charité artificial disc on the implanted and adjacent spinal segments mechanics using a hybrid testing protocol. Spine. 2005;30:2755-64.
[72] Grauer, JN, Biyani A, Faizan A, et al. Biomechanics of two-level Charite artificial disc placement in comparison to fusion plus single-level disc placement combination. Spine J. 2006;6:659-66.
[73] Panjabi MM, Henderson G, James Y, et al. StabilimaxNZ versus simulated fusion: evaluation of adjacent-level effects. Eur Spine J. 2007;16:2159-65.
[74] Zhang QH, Teo EC. Finite element application in implant research for treatment of lumbar degenerative disc disease. Med Eng Phys. 2008;30:1246-56.
[75] Jones AC, Wilcox RK. Finite element analysis of the spine: Toward a framework of verification, validation and sensitivity analysis. Med Eng Phys. 2008;30:1287-304.
[76] Lu YM, Hutton WC, Gharpuray VM. Do bending, twisting, and diurnal fluid change in the disc affect the propensity to prolapse? A viscoelastic finite element model. Spine. 1996;21:2570-9.
[77] Goel VK, Monroe BT, Gilbertson LG, et al. Interlaminar shear stresses and laminae separation in a disc. Finite element analysis of the L3-L4 motion segment subjected to axial compressive loads. Spine. 1995;20:689-98.
[78] Rohlmann A, Zander T, Bergmann G. Effects of total disc replacement with ProDisc on intersegmental rotation of the lumbar spine. Spine. 2005;30:738-43.
[79] Schmidt H, Heuer F, Simon U, et al. Application of a new calibration method for a three-dimensional finite element model of a human lumbar annulus

fibrosus. Clin Biomech. 2006;21:337-44.

[80] Polikeit A, Ferguson SJ, Nolte LP, et al. Factors influencing stresses in the lumbar spine after the insertion of intervertebral cages: finite element analysis. Eur Spine J. 2002;12:413-20.

[81] Shirazi-Adl A, Ahmed AM, Shrivastava SC. Mechanical response of a lumbar motion segment in axial torque alone and combined with compression. Spine. 1986;11:914-27.

[82] Agur AMR, Lee MJ. Grant's atlas of anatomy, 10th edition, Lippincott Williams & Wilkins, Philadelphia, Pennsylvania, 1999.

[83] White AA, Panjabi MM. Clinical biomechanicals of the spine. 2nd edition, J.B. Lippincott Company, Philadelphia, Pennsylvania 1990.

[84] Lee KK, Teo EC, Fuss FK, et al. Finite-element analysis for lumbar interbody fusion under axial loading. IEEE Trans. Biomed Eng 2004;51:393-400.

[85] Liau, Hu CC, Cheng CK. The inference of interesting a Fuji pressure sensitive film between the tibiofemoral joint of knee prosthesis on actual characteristics. Clin Biomech. 2001;16:160-6.

[86] Yamamoto I, Panjabi MM, Crisco T, et al. Three-dimension movement of the whole lumbar spine and lumbosacral joint. Spine. 1989;14:1256-60.

[87] Godest AC, Beaugonin M, Haug E, et al. Simulation of a knee joint replacement during a gait cycle using explicit finite element analysis. J Biomech. 2002;35:267-75.

[88] Chen CS, Cheng CK, Liu CL, et al. Stress analysis of the disc adjacent fusion in lumbar spine. Med Eng Phys. 2001;23:483-91.

[89] Panjabi MM, Oxland TR, Yamamoto I, et al. Mechanical behavior of the human lumbar and lumbosacral spine as shown by three-dimensional load-displacement curves. J. Bone Joint Surg Am. 1994;76:413-24.

[90] Rohlmann A, Neller S, Claes L, et al. Influence of a follower load on intradiscal pressure and intersegmental rotation of the lumbar spine. Spine.

2001;26:E557-61.
[91] Shirazi-Adl A. Nonlinear stress analysis of the whole lumbar spine in torsion-mechanics of facet articulation. J Biomech. 1994;27:289-99.
[92] Eberlein R, Holzapfel A, Frohlich M. Multi-segment FEA of the human lumbar spine including the heterogeneity of the annulus fibrosus. Comput Mech. 2004;34:147-63.
[93] Oxland TR, Lund T. Biomechanics of stand-alone cages and cages in combination with posterior fixation: a literature review. Eur Spine J. 2000;9:S95-101.
[94] Gerber M, Crawford NR, Chamberlain RH, et al. Biomechanical assessment of anterior lumbar interbody fusion with an anterior lumbosacral fixation screw-plate: Comparison to stand-alone anterior lumbar interbody fusion and anterior lumbar interbody fusion with pedicle screws in an unstable human cadaver model. Spine. 2006;31:762-8.
[95] Panjabi MM, Henderson G, Abjornson C, et al. Multidirectional testing of one- and two-level ProDisc-L versus simulated fusions. Spine 2007;32:1311-9.
[96] Panjabi MM, Malcolmson G, Teng E, et al. Hybrid testing of lumbar CHARITE discs versus fusions. Spine. 2007;32:959-66.
[97] Zhong ZC, Chen SH, Chen WJ, et al. Comparison of the load and displacement controlled finite element analyses on fusion and non-fusion spinal implants. J Biomech. 2007;40:S353.
[98] Dick JC, Jones MP, Zdeblick TA, et al. A biomechanical comparison evaluating the use of intermediate screws and cross-linkage in lumbar pedicle fixation. J Spinal Disord. 1994;7:402-7.
[99] Chutkan NB, Zhou H, Akins JP, et al. Effects of facetectomy and crosslink augmentation on motion segment flexibility in posterior lumbar interbody fusion. Spine. 2008;33:E828-35.
[100] Tropiano P, Huang RC, Girardi FP, et al. Lumbar disc replacement: Preliminary results with ProDisc II after a minimum follow-up period of 1 year.

J Spinal Disord Tech. 2003;16:362-8.
[101] Lemaire JP, Carrier H, Sariali el-H, et al. Clinical and radiological outcomes with the Charite artificial disc: a 10-year minimum follow-up. J Spinal Disord Tech. 2005;18:353-9.
[102] van Ooij A, Cumhur Oner F, Verbout ABJ. Complications of artificial disc replacement: A report of 27 patients with the SB Charite' disc. J Spinal Disord Tech. 2003;16:369-83.
[103] Punt IM, Visser VM, van Rhijn LW, et al. Complications and reoperations of the SB Charité lumbar disc prosthesis: experience in 75 patients. Eur Spine J. 2008;17:36-43.
[104] Dooris AP, Goel VK, Grosland NM, et al. Load-sharing between anterior and posterior elements in a lumbar motion segment implanted with an artificial disc. Spine. 2001;26:E122-9.
[105] Rundell SA, Auerbach JD, Balderston RA, et al. Total disc replacement positioning affects facet contact forces and vertebral body strains. Spine. 2008;33:2510-17.
[106] Rohlmann A, Zander T, Bock B, et al. Effect of position and height of a mobile core type artificial disc on the biomechanical behaviour of the lumbar spine. Proc Inst Mech Eng H. 2008;222:229-39.
[107] Chung SK, Kim YE, Wang KC. Biomechanical effect of constraint in lumbar total disc replacement: A study with finite element analysis. Spine. 2009;34:1281-6.
[108] Mulholland RC, Sengupta DK. Rationale, principles and experimental evaluation of the concept of soft stabilization. Eur Spine J. 2002;11:S198-205.
[109] Panjabi MM, Goel V, Oxland T, et al. Human lumbar vertebrae quantitative three-dimensional anatomy. Spine. 1992;17:299-306.
[110] Panjabi MM, Oxland T, Takata K, et al. Articular facets of the human spine. Quantitative three-dimensional anatomy. Spine. 1993;18:1298-310.
[111] Nachemson A. Lumbar intradiscal pressure. In The lumbar spine and back

pain (Ed M.I.V Jayson), pp. 191-203, Churchill Livingstone, Edinburgh, 1987.
[112] Qunit U, Wilke HJ, ShiraziAdl A, et al. Importance of the intersegmental trunk muscles for the stability of the lumbar spine. A biomechanical study in vitro. Spine. 1998;23:1937-45.
[113] Patwardhan AG, Havey RM, Meade KP, et al. A follower load increases the load-carrying capacity of the lumbar spine in compression. Spine. 1999;24:1003-9.

Publication List

Journal Papers:

1. Liu CL, **Zhong ZC**, Shih SL, Hung C, Lee YE, Chen CS. Influence of Dynesys system screw profile on adjacent segment and screw. *Journal of Spinal Disorders & Techniques* 2008. (Accepted)
2. **Zhong ZC**, Chen SH, Hung C. Load- and displacement- controlled finite element analyses on fusion and non-fusion spinal implants. *Proceedings of the Institution of Mechanical Engineers, Part H - Journal of Engineering in Medicine* 2009 Feb; 223(2):143-157.
3. Chen SH, **Zhong ZC**, Chen CS, Chen WJ, Hung C. Biomechanical comparison between lumbar disc arthroplasty and fusion. *Medical Engineering & Physics* 2009 Mar; 31(2):244-253.
4. Chiang MF, **Zhong ZC**, Chen CS, Cheng CK, Shih SL. Biomechanical comparison of instrumented posterior lumbar interbody fusion with one or two cages by finite element analysis. *Spine* 2006 Sep; 31(19): E682-E689.
5. Wang JP, **Zhong ZC**, Cheng CK, Chen CS, Yu Ch, Chang TK, Wei SH. Finite element analysis of the spondylolysis in lumbar spine. *Bio-Medical Materials & Engineering* 2006 Oct; 16(5):301-308.
6. **Zhong ZC**, Wei SH, Wang JP, Feng CK, Chen CS, Yu Ch. Finite element analysis of the lumbar spine with a new cage using topology optimization method. *Medical Engineering & Physics* 2006 Jan; 18(1):90-98.
7. Chen SH, Chiang MC, **Zhong ZC**, Hung C. The finite element analysis using a follower load on fusion and non-fusion spinal implants. *Journal of Orthopaedic Surgery Taiwan* 2009. (Accepted)
8. Chen SH, Chao SH, **Zhong ZC**, Hung C. Biomechanical comparison of two new stand-alone anterior lumbar interbody fusion cages (SynFix and Stabilis) with established fixation techniques – a three-dimensional finite element analysis. *Journal of Orthopaedic Surgery Taiwan* 2009. (Accepted)

Conference Papers:

1. Chen SH, Chao SH, **Zhong ZC**, Hung C, Chen WJ. Biomechanical comparison of unilateral and bilateral pedicle screws fixation for transforaminal lumbar interbody interbody fusion after decompressive surgery - A finite element analysis. *Orthopaedic Research Society 55th Annual Meeting* (ORS 55th), No. 1725, Las Vegas, Nevada, US (February 22-25, 2009)

2. **Zhong ZC**, Chen SH, Chen WJ, Hung C. Comparison of the load and displacement controlled finite element analyses on fusion and non-fusion spinal implants. *International Society of Biomechanics XXI Congress* (21st ISB 2007), Taipei, Taiwan (July 1-5, 2007) Published in *Journal of Biomechanics* 2007;40(S2):S353.
3. **Zhong ZC**, Chiang MF, Hung C, Chen CS, Cheng CK. Biomechanical comparison of instrumented lumbar interbody fusion with one or two cages by finite element analysis. *The 2nd Asian Pacific Conference On Biomechanics* (APB2005), Taipei, Taiwan (November 23-25, 2005)
4. 陳世豪、江銘傑、**鍾政成**、陳文哲、洪景華，應用伴隨負荷之有限元素模型對融合與非融合腰椎植入物之分析比較，台灣脊椎外科醫學會 98 年度會員大會暨學術研討會，台北。(March 13-15, 2009)
5. 陳世豪、趙時恆、**鍾政成**、羅正展、洪景華，減壓手術時 TILF 搭配使用單側或雙側椎足螺釘系統之生物力學特徵比較–有限元素模擬分析，台灣脊椎外科醫學會 98 年度會員大會暨學術研討會，台北。(March 13-15, 2009)
6. Chen SH, **Zhong ZC**, Chiang MC, Chen WJ, Hung C. The load and displacement controlled finite element analyses with follower load on fusion and non-fusion spinal implants. *55th Congress of Taiwan Orthopaedic Association*, Taoyuan, Taiwan (October 25-26, 2008)
7. Chen SH, Chao SH, **Zhong ZC**, Lo CC, Hung C. Biomechanical comparison of two new stand-alone anterior lumbar interbody fusion cages (SynFix and Stabilis) with estabilished fixation techniques – a three-dimensional finite element analysis. *55th Congress of Taiwan Orthopaedic Association*, Taoyuan, Taiwan (October 25-26, 2008)
8. Chen SH, Lo CC, Tsai KJ, **Zhong ZC**, Hung C. Biomechanical effect of interspinous process decompression device Coflex after decompression surgery. *54th Congress of Taiwan Orthopaedic Association*, Taichung, Taiwan (April 19, 2008)
9. Chen SH, **Zhong ZC**, Chiang MC, Chen WJ, Hung C. The load and displacement controlled finite element analyses on fusion and non-fusion spinal implants. *53rd Congress of Taiwan Orthopaedic Association*, Taoyuan, Taiwan (October 27-28, 2007).
10. Chen SH, Hsu PF, **Zhong ZC**, Lo CC, Chen WJ, Hung C. Biomechanical comparison between transforaminal and posterior lumbar interbody fusion devices after decompressive surgery. *53rd Congress of Taiwan Orthopaedic Association*, Taoyuan, Taiwan (October 27-28, 2007).
11. Chen SH, **Zhong ZC**, Chen WJ, Hung C. Biomechanical comparison between artificial disc and lumbar interbody fusion devices. *52nd Congress of Taiwan Orthopaedic Association Combine The 15th Annual Meeting of Taiwan Spine Society*, Kaohsiung, Taiwan (April 28, 2007).

Patient:

1. **鍾政成**、陳振昇、王榮彬，脊椎骨融合假體/prosthetic cage for spinal fusion，中華民國新型專利第 M273326 號。中華民國專利公報 V32，N24，**(2005)**

Vita

個人簡介

中文姓名	鍾政成
英文姓名	Zhong, Zheng-Cheng
性別	男
出生日期	民國 69 年 2 月 23 日
聯絡電話	0952373927
E-mail	zczhong2002@yahoo.com.tw ; zc.zhong@msa.hinet.net
地址	412 台中縣大里市益民路一段 503 號

學歷

學校名稱	國別	主修學門系所	學位	起訖年月(西元年/月)
國立交通大學	中華民國	機械工程學系	博士	2004 / 09~2009 / 08
國立陽明大學	中華民國	復健科技輔具所	碩士	2002 / 09~2004 / 06
國立虎尾科技大學	中華民國	動力機械工程學系	學士	2000 / 09 ~2002 / 06

學會會員

1. Taiwan Society of Biomechanics (TSB) 2007/Apr
2. International Society of Biomechanics (ISB) 2006~